49. Peirson, A., *Brit. J. Appl. Phys.*, 6, 444 (1955).
50. Peirson, D. H., and Iredale, P., *Brit. J. Appl. Phys.*, 8, 422 (1957).
51. Iredale, P., *AERE-EL/M*-108 (1960).
52. Adams, F., and Hoste, J., *Talanta*, 9, 827 (1962).
53. De Soete, D., and Hoste, J., *I.A.E.A., Radiochem. Meth. of Anal.*, Salzburg, Proc. II, p. 91 (1964).
54. De Soete, D., and Hoste, J., *Nature*, 194, 859 (1962).
55. De Soete, D., and Hoste, J., *Radiochim. Acta*, 4, 35 (1965).
56. Gijbels, R., and Hoste, J., *Anal. Chim. Acta*, 29, 280 (1963).
57. Gibbons, D., Fite, L. E., and Wainerdi, R. E., *Anal. Chem.*, 34, 269 (1962).
58. Kuykendall, W. E., Wainerdi, R. E., and associates; I.A.E.A. *Use of Radioisotopes in the Phys. Sci. and Ind.*, Copenhagen RICC/198 (1960).
59. Wainerdi, R. E., and du Beau, N. P., *Science*, 139, 1027 (1963).
60. Wainerdi, R. E., Fite, L. E., Gibbons, D., Wilkins, W. W., Jiminez, P. and Drew, D., I.A.E.A., *Radiochem. Meth. of Anal.*, Salzburg, Proc. II, p. 149 (1964).
61. Drew, D., Fite, L. E., and Wainerdi, R. E., *Nucl. Sci. Series Rept.* NAS-NS 3107, p. 237 (1962).
62. Wainerdi, R. E., Fite, L. E., and Steele, L. E., 3e Congrès Int. de Biologie de Saclay, Comptes-rendus, p. 171 (1963).
63. Hoste, J., De Soete, D., and Speecke, A., *Euratom Rept.*, EUR 3565e (1967).
64. Comar, D., and Le Poec, C., *Mod. Trends in Act. Anal.*, Texas, Proc. p. 351 (1965).
65. Comar, D., and Le Poec, C., I.A.E.A. *Radiochem. Meth. of Anal.*, Salzburg, Proc. II, p. 15 (1964).

CHAPTER 10

SYSTEMATIC ERRORS IN ACTIVATION ANALYSIS

I. General Considerations

The activity induced in an element after an irradiation time t_b can be calculated from equation (5.36), in the case of "simple activation". A more practical form of this equation is

$$R(t_b) = \frac{wz\theta N_A \sigma \varphi y}{A}\left[1 - \exp\left(\frac{-0.693\, t_b}{T_{1/2}}\right)\right] \qquad (10.1)$$

$R(t_b)/3.7 \times 10^7$ gives the activity in millicurie (mc). After a waiting time t, the activity is obviously given by equation (5.37):

$$R(t_b, t) = R(t_b) \exp\left(-0.693\, t/T_{1/2}\right) \qquad (10.2)$$

In the case of more complex systems, including isomeric activation, parent-daughter relationships, etc. equations (5.44), (5.47), (5.52), (5.53), (5.55), (5.56), (5.59), (5.60) ... or their practical equivalents should be used. In the above equations:

- R = measured activity in cps ($R = zD$, where D = disintegration rate in dps);
- w = weight of the irradiated element in gram; (if a compound, such as an oxide, is irradiated, its weight must be multiplied with the appropriate analytical conversion factor);
- z = efficiency of the detector;
- θ = abundance of the activated nuclide (100% = 1);
- A = atomic weight of the irradiated element;
- N_A = Avogadro's number = 6.023×10^{23};
- y = chemical yield (if the activity is counted after a chemical separation);
- $T_{1/2}$ = half-life of the radionuclide formed;
- t_b and t = irradiation and waiting time respectively; (expressed in the same unit as $T_{1/2}$: s, m, h ...);
- σ = isotopic activation cross section. If only thermal activation occurs (i.e. at the irradiation position the cadmium ratio of

the nuclide is high, say ≥ 50), $\sigma = \sigma_{th}$ (it can be proved that $\sigma_{th} \simeq \sigma_0$ (2200 m/s cross section).

φ = neutron flux in n cm^{-2} s^{-1} (in most cases $\varphi_{th} \approx \varphi_{reactor}$, as normally at least 95% of the neutrons are thermal).

The exact nature of σ_{th} has been explained by Stoughton and Halperin (1). For any nuclide the value of σ_{th} depends slightly on φ_e/φ_{th} as well as on the thickness of the Cd-shield used to determine σ_{th}. The tabulated (n, γ) cross sections (D. J. Hughes (2); Appendix 1, Table 2) are in most cases for neutrons with 2200 m/s velocities, usually denoted by σ_0. For most nuclides σ_0 approximates σ_{th} very closely and can be substituted for σ_{th} in neutron flux equations with only a small error. The authors described how σ_{th} can be calculated if σ_0 and some experimental parameters are known.

If resonance activation is not negligible, σ is expressed in terms of a "reactor" cross section: $\sigma_{reactor} = g\sigma_0 + (\varphi_e/\varphi_{th})I$, where I = total activation resonance integral for the nuclide of interest ($I = I' + 0.44\ \sigma_0$, where the latter term is the $1/v$ contribution to the resonance integral,) φ_{th} = thermal flux (Maxwellian distribution); φ_e = epithermal or resonance flux (dE/E component with a low-energy cut-off at ca. 0.5 eV). In most cases $g = 1$ (Table 10.1).

TABLE 10.1

g-values for some elements after H. Rose *et al.* (3)

Be, Al, Co, Zn, Mo, Cs, Pb, Na, V, Ni, Zr, Sn, Ta, Bi, Mg, Fe, Cu, Nb, Te, Pt	$g = 1$
Cd	$g = 1.321$
In	$g = 1.017$
Sm	$g = 1.620$
Gd	$g = 0.893$
Au	$g = 1.005$

If a radionuclide is formed by a (n, p) or (n, α) reaction in a reactor, $\varphi = \bar{\varphi}$ and obviously $\sigma = \bar{\sigma}$ (n, p) or $\bar{\sigma}$ (n, α), (see Chapter 3; methods for determining the thermal, epithermal and fast flux in a reactor are described in the same chapter). If a radionuclide is formed by a (n, p), (n, α) or (n, 2n) reaction during 14 MeV activation, $\varphi = F$ (14 MeV flux) and $\sigma = \sigma_{14\ MeV}$.

After counting the induced activity, equations (10.1) or (10.2) allow in theory the calculation of the weight w of the element present in the sample. In the case of "absolute" activation analysis this is actually done. However, some parameters must be known, such as the absolute value of the conventional thermal flux (accuracy ±5% according to Hughes), the value of the cadmium ratio (this value being either directly or indirectly required to obtain the absolute value of the thermal flux; accuracy estimated ±2% (4)), the irradiation time (this factor being significant for short irradiation times, ±3% (4)), the half-life (average error ±2% if 0.5 d < $T_{1/2}$ < 10 d; ±3% if 15 d < $T_{1/2}$ < 60 d; ±11% if 0.5 y < $T_{1/2}$ < 4 y, with exceptions, of course, such as ^{60}Co, ±0.7% (4)); the decay schemes, including the ratio e/γ, branching ratios, etc. (errors between ±2 and ±50% (4)), the thermal activation cross section (from ±5 up to ±30% for a large number of (n, γ) reactions (4)), the counter calibration (in the case of γ counting ±1.5 to ±4.5% (4)).

Fast neutron cross sections and average cross sections in a fission neutron spectrum are even less well known and often differ by up to a factor of 10.

In practice a relative method is normally followed which eliminates the foregoing uncertainties inherent in the absolute method. A known amount w_s of the element to be determined is irradiated together with the sample as a flux monitor (comparator). From the ratio of the induced activities in the unknown sample (A_x) and in the standard (A_s), the weight w_x of the element of interest in the sample can be readily calculated from

$$w_x/w_s = A_x/A_s \qquad (10.3)$$

on condition that all the other parameters (θ, z, σ, φ) are identical and that the radionuclide is not formed from another nuclide in the sample (interfering reactions). If this condition is not fulfilled, errors are possible, which will be discussed below.

II. Sources of Error Using the Comparator Method

(A) Anomalous Isotopic Abundances

Variations in the boron isotopic abundances with samples of different origin as high as 3–4% have been reported by Thode *et al.* (5). This

has an important consequence in terms of the use of boron as a standard in precise measurements of neutron capture cross sections, since the ^{10}B content, on which these measurements are based, is not rigorously constant.

Measurements carried out by Thode (6) with sulfur from different sources (native sulfur, pyrites, natural sulfates, hydrothermal sulfides, etc.) also showed differences of approximately 4% in the $^{32}S/^{33}S$ ratio and of 8% in $^{32}S/^{34}S$, due to fractionations by physicochemical and biochemical processes. Natural variations of several per cent in the relative isotopic abundance of ^{48}Ca in samples of diverse geological origin have been found (7). Other elements which can have anomalous isotopic ratios are Ar, Sr, Sn, Ba, Ce, Nd, Yb, Hf, Os, Tl, Pb and the heavier elements (8).

Sautin (9) found that the isotopic abundance of ^{152}Gd in a gadolinium standard was different from that in a didymium sample, probably due to fractionation on an ion-exchange column used for the purification of the standard. Even if the fractionation is small for the natural isotopes as a whole, it can be relatively important if the activation analysis is based on ^{153}Gd, as ^{152}Gd has a natural abundance of 0.2% only. Indeed, an error of 50% was observed if the results were compared with analyses based upon ^{159}Gd or ^{161}Tb.

Isotopic ratios of some elements like U, Li, B have intentionally been modified in recent years on a large scale, with the aim of preparing samples enriched in certain isotopes. Besides the expensive enriched mixtures, the depleted ones are also sold and often without adequate warning that the product concerned is of a different isotopic composition. De Goeij *et al.* (10) measured Li isotope ratios in a number of commercial preparations. Out of 9 samples investigated, 4 had a very abnormal isotopic composition. The results were 0.98 – 0.98 – 1.00 – 0.98 – 0.87 – 1.16 (1.19) – 1.44 (1.54) – 2.53 (2.60) – 2.94 for the $^{7}Li/^{6}Li$ ratio; the values between brackets were determined by activation analysis according to Born and Aumann (11) combined with flame photometry; the other values by mass spectrometry. Another typical example is uranium. This element can be determined by the reaction $^{235}U(n, f)^{140}Ba$ (suitable fission product) or by the reaction $^{238}U(n, \gamma)^{239}U \xrightarrow{\beta^-} {}^{239}Np$. When the standard has the same isotopic composition as the uranium in the sample, both methods will give correct results.

(B) Errors Due to Different Fluxes in Samples and Standards

The main source of error is due to the fact that standard and sample are not exposed to the same neutron flux, i.e. $\varphi(s) \neq \varphi(x)$.

(1) Neutron flux variations are possible as a function of time. For that reason standards and samples are irradiated simultaneously, or an internal standard, as proposed by Leliaert *et al.* (12), is used for normalizing all the irradiations to the same flux.

(2) Of more importance than time stability are flux variations as a function of irradiation position and for that reason standard and samples are irradiated together in one irradiation can. In the large core of a graphite-moderated reactor, the neutron flux varies slowly with distance (max. ca. 0.5%/cm), ensuring that the flux reaching the sample and standard is the same (error <2%). Near the reflector however (highest "cadmium ratio") the flux may vary by as much as 2–3%/cm; as sample and standard may be separated by as much as a few cm, considerable errors are possible. It is then necessary to make sure that the sample and standard are as close together as possible (13,14). Difficulties with an inhomogeneous flux can be overcome by irradiating the targets one after another and using a small flux monitor attached to a fixed position in the irradiation can or "rabbit", particularly in the case of short irradiations.

In the case of more compact small-core water-moderated reactors, still higher flux gradients are observed with distance from the core and gradients of 10%/cm are possible (15). To correct for flux gradients in the material testing reactor BR–2, De Neve (16) surrounded samples (A, B) and standards (I, II, III) in an aluminium block with cobalt needles (1 to 6) as flux monitors (Figure 10.1).

From nos. 1, 2 and 3 the average flux for sample A was calculated, from nos. 1, 3 and 4 the average flux for standard I, etc. Flux gradients of 0 to 9%/cm (average gradient 3%/cm) were observed, as appears from Table 10.2, where the thermal flux for the irradiation places 1 to 6 is given for three different irradiations.

Even in the case of an apparent low flux gradient, flux variations are possible if strong neutron absorbers are placed near the activation position. This can give rise to deep flux depressions and hence to a steep unknown flux gradient in the activation tube (see further: definition of flux perturbation, flux depression and self-absorption). It is obvious, that $\sigma_{reactor}$ will not be constant for all the samples and

TABLE 10.2
Thermal flux for irradiation positions 1 to 6 (Fig. 10.1)

Flux monitor	t_b = 10 h	t_b = 15 h	t_b = 20 h
1	0.92 × 10^{14}	1.00 × 10^{14}	5.48 × 10^{13}
2	0.95	1.00	5.45
3	0.93	0.98	5.90
4	0.93	—	5.72
5	0.93	1.06	5.28
6	0.95	1.06	5.14

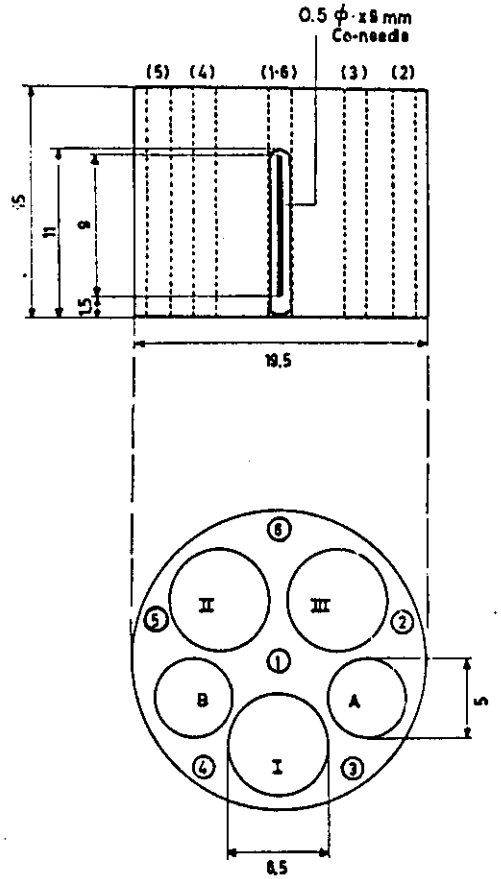

Fig. 10.1. Irradiation block which permits correction for flux gradients (16). 1-6: cobalt needle flux monitors; I–III: standards; A–B: samples.

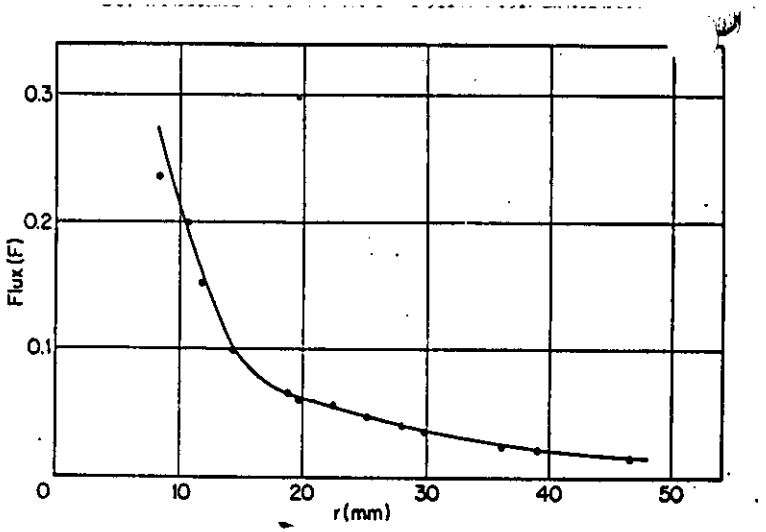

Fig. 10.2. Fast neutron flux pattern for a 14 MeV neutron generator: Axial flux distribution (20).

standards, if they are irradiated at a reactor position, where the cadmium ratio changes rapidly with the space coordinates.

Flux gradients are even more important in fast neutron activation analysis. Experimental data are given by Lepetit (17), Mott (18) and Kenna (19).

14 MeV neutrons are produced by deuteron bombardment of a tritiated titanium target (diameter 15 to 30 mm). Flux variations in the samples are primarily due to geometrical factors. Op de Beeck (20) calculated the axial flux distribution as a function of the distance r from the target and found agreement with experimental values determined by means of copper foils of 0.4 mm thickness (Figure 10.2). The relative flux as a function of distance a across planes parallel to target is presented in Figure 10.3, for any distance r normalizing to $F = 1$ (20).

From Figure 10.2 appears that at $r = 10$ mm an axial displacement of 1 mm corresponds to a flux variation of ca. 14% in the sample. At $r = 18$ mm this value is ca. 8.5%. Transversal displacements d can also induce considerable errors, as appears from Figure 10.3. Similar results were found by Girardi *et al.* (21). Moreover, irregularities in the described flux are possible due to scattering or to a nonuniformly loaded or depleted target (19).

(3) Another factor that can cause variation of the flux within an irradiation unit is neutron attenuation by different sample-packing materials (14).

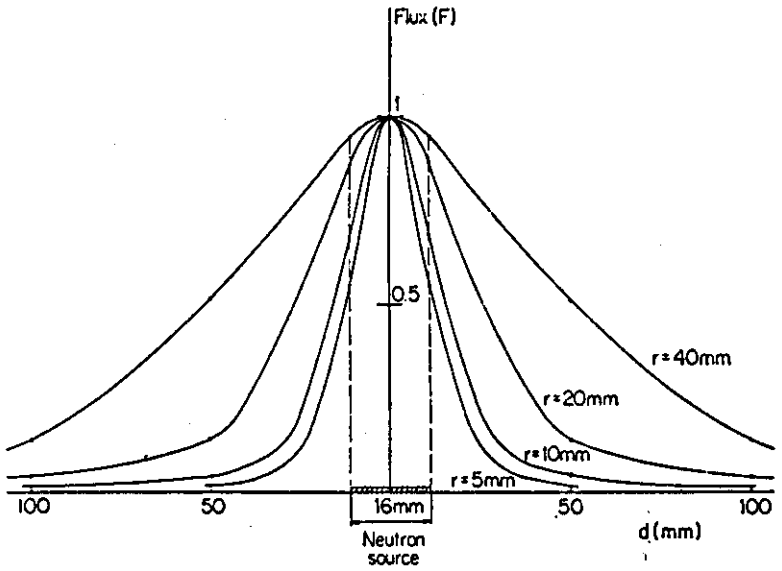

Fig. 10.3. Fast neutron flux pattern for a 14 MeV neutron generator: Transversal flux distribution (20).

(4) Attenuation of the neutron flux by the samples or standards themselves makes the inside part less active than the outside. This can directly be seen from Figure 10.4, where the induced specific activity in subsequent shells of an antimony sphere is represented as a function of depth (22). Consequently, the specific activity will decrease with the sample size, this being a measure for the neutron absorption in the sample (viz. standard).

If this effect is different in standards and samples, $\varphi(s) \neq \varphi(x)$ and equation (10.3) is again not valid. As appears from Figure 10.4 the shielding effect in antimony spheres depends on the neutron spectrum. Whereas for a $CR_{Au} = 155$ no shielding effect is observed, it is very important for a $CR_{Au} = 5.5$, indicating resonance absorption in ^{121}Sb and ^{123}Sb.

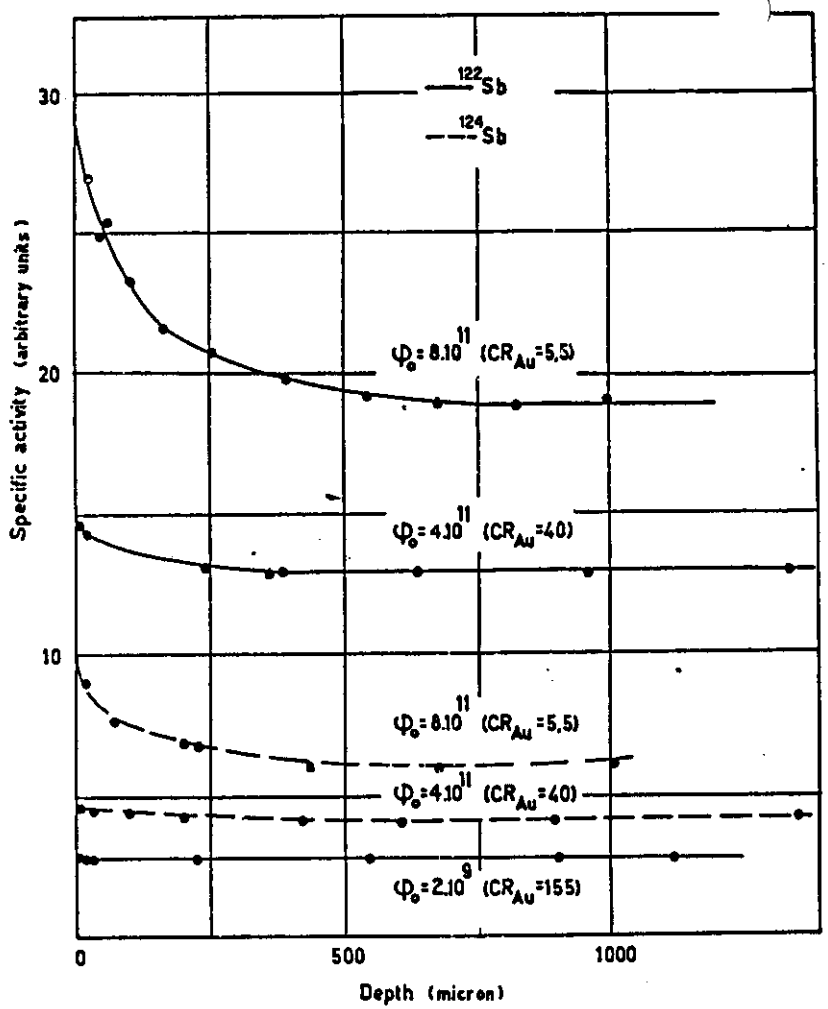

Fig. 10.4. Specific activity of ^{122}Sb and ^{124}Sb in subsequent layers of antimony spheres (22).

Some effects, causing $\varphi(s) \neq \varphi(x)$, are schematically shown in Figure 10.5.

(a) **Definitions.** As much confusion exists concerning self-absorption, flux depression and flux perturbation, it can be useful to point out the differences between these concepts (23). When an absorber is

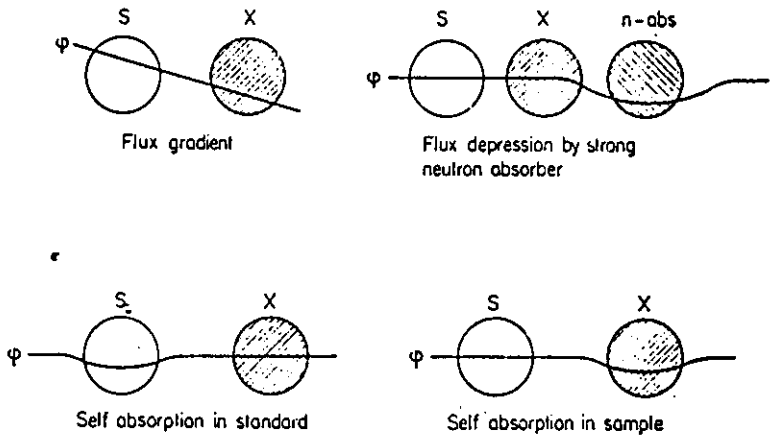

Fig. 10.5. Neutron flux differences in standards and samples.

placed in a diffusing medium, the neutron flux will be perturbated inside and outside the sample (Figure 10.6). In the vicinity of the absorber a flux gradient exists such that the neutron flux decreases towards the sample. This effect is called flux depression and is due to the fact that neutrons which are absorbed in the sample are unable to scatter back into the moderator so as to maintain a constant neutron flux.

The neutron flux decreases inside the sample because neutrons are removed by absorption. This effect is called self-absorption. The total effect of flux depression + self-absorption is called flux perturbation. If the unperturbated flux is represented by φ, the average flux over the

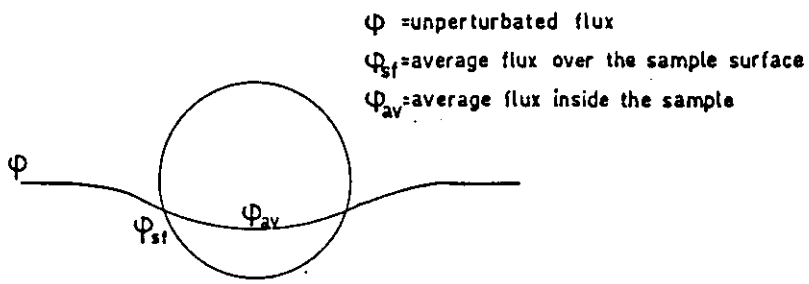

Fig. 10.6. Flux perturbation, flux depression and self-absorption.

surface of the sample by φ_{sf} and the average flux inside the sample by φ_{av} the three factors mentioned can be defined as follows:

flux depression factor φ_{sf}/φ

self-absorption factor $\varphi_{av}/\varphi_{sf}$

flux perturbation factor φ_{av}/φ

For practical purposes in activation analysis, a factor f will be defined (equation (10.10)) which is only an estimate of the absorption effect. An accurate theoretical treatment of the three separate factors above is indeed too difficult.

Several calculation and approximation methods to correct for neutron shielding are described in the literature (24–29). In most cases they are only valid if resonance absorption is negligible, i.e. that the nuclide of interest has a high cadmium ratio at the irradiation position used (see further). If this condition is not fulfilled a distinction must be made between two cases: (a) self-absorption in the standard (one element) or (b) in the sample (more elements): the element being determined is usually – though not always – present in a low enough concentration for self-shielding effects to be negligible, even if it has a very high absorption cross-section. Self shielding is therefore only likely when strongly absorbing major constituents occur in the matrix or when the matrix itself has a high absorption cross section: in this case the neutron absorption will influence the activity induced in the trace constituents.

These problems are discussed in detail by Høgdahl (23, 30).

(b) Calculations according to Høgdahl (reactor activation). The convention of Høgdahl will be followed in the next discussion, including the simplification that most nuclides in reactor neutron activation have absorption cross sections that follow the "1/v law" (see Chapter 3). For 14-MeV neutrons: see section II, B, 3(b) of this chapter (remark).

(1) *Calculation of total absorption effect.* For these nuclides the reaction rate per atom for a substance at high dilution or in very small amounts, including both thermal and epithermal (but not fast*) reactions can be written:

$$R = R_{th} + R_e = n_{th} v_0 \sigma_0 + \varphi_e I = n_{th} v_0 \sigma_{reactor} \qquad (10.4)$$

*The contribution to the total (n, γ) reaction rate, due to fission neutrons being negligible.

where

$$\sigma_{\text{reactor}} = \sigma_0 + \frac{\varphi_e}{n_{\text{th}} v_0} \tag{10.5}$$

n_{th} = neutron density for energies up to Cd cut-off (E_{Cd})
v_0 = 2200 m s^{-1}
σ_0 = 2200 m s^{-1} cross section
φ_e = epicadmium flux ($> E_{\text{Cd}}$)
I = the infinite dilute resonance integral = $\int_{E_{\text{Cd}}}^{1\text{ MeV}} \frac{\sigma(E)}{E}\,dE$

(I contains the "1/v-tail", the latter being 0.44 σ_0) (*cf.* section V, C, 2 of Chapter 3).

The ratio $\varphi_e/n_{\text{th}}v_0$ (or $\varphi_e/\varphi_{\text{th}}$) can be determined by irradiating appropriate monitors with and without cadmium cover, i.e. by determining the cadmium ratio $CR = (n_{\text{th}}v_0\sigma_0 + \varphi_e I)/\varphi_e I$ (see Chapter 3).

The disintegration rate of the nuclides at the end of the irradiation is given by

$$D = \frac{w}{A}\,\theta N_A\,\sigma_{\text{reactor}} v_0 n_{\text{th}}\,[1 - \exp(-\lambda t_b)] \tag{10.6}$$

assuming that there is no absorption effect.

If neutrons are absorbed by the substance, the above equations must be modified.

Reaction rate inside an irradiated sample:

$$R' = R'_{\text{th}} + R'_e.$$

It can be shown that $R'_{\text{th}} = \bar{n}_{\text{th}} v_0 \sigma_0$ ($\bar{n}_{\text{th}}$ being the average thermal neutron density inside of the sample, assuming a "1/v-law" for σ_{abs} up to E_{Cd}.

It is difficult to write down a general expression for R'_e as a function of the neutron density inside a sample. It can, however, be written in terms of an effective resonance integral I^{eff}, defined by $R'_e = \varphi_e I^{\text{eff}}$. Hence:

$$R' = \bar{n}_{\text{th}} v_0 \sigma_0 + \varphi_e I^{\text{eff}} = \bar{n}_{\text{th}} v_0 \sigma^{\text{eff}}_{\text{reactor}} \tag{10.7}$$

where:

$$\sigma^{\text{eff}}_{\text{reactor}} = \sigma_0 + \frac{\varphi_e}{\bar{n}_{\text{th}} v_0} I^{\text{eff}} \tag{10.8}$$

thus:

$$D' = \frac{w}{A}\,\theta N_A\,\sigma^{\text{eff}}_{\text{reactor}} v_0 \bar{n}_{\text{th}}\,[1 - \exp(-\lambda t_b)] \tag{10.9}$$

From the ratio D'/D a total "absorption" factor f can be defined for the nuclide in question (equations (10.9), (10.6))

$$f = \frac{\sigma^{\text{eff}}_{\text{reactor}} \bar{n}_{\text{th}}}{\sigma_{\text{reactor}} n_{\text{th}}} = f_{\text{th}} \frac{R_{\text{th}}}{R} + f_e \frac{R_e}{R} = \left(1 - \frac{1}{CR}\right) f_{\text{th}} + \frac{1}{CR} f_e \tag{10.10}$$

where CR = the cadmium ratio for the nuclide of interest, of which the activity is measured;
f_{th} = the thermal absorption factor, defined by $\bar{n}_{\text{th}}/n_{\text{th}}$ (= $R'_{\text{th}}/R_{\text{th}}$);
f_e = the epicadmium absorption factor, defined by I^{eff}/I. (R'_e/R_e in the empirical approach of Reynolds and Mullins (31)); R'_e/R_e is described as the average resonance flux within the sample divided by that value, if the sample were absent, see equation (10.22).

If the neutron absorption is only due to a nuclide which is a main constituent of a sample, the absorption factors f, f_{th} and f_e are true self-shielding factors. Note that from equation (10.10) it appears that the contribution of epithermal neutron absorption to the total absorption depends on the degree of thermalization of the neutrons, i.e. on the cadmium ratio for the nuclide of interest (*cf.* Figure 10.4).

(2) *Thermal absorption, thermal flux enhancement and flux hardening.* The thermal absorption can be computed reasonably accurately using equations given by Zweifel (26), on condition that $\bar{\sigma}_s/\sigma_T < 0.1$ (32). Analogous relationships are formulated by other authors (24–29). The calculation of f_{th}, taking into account the neutron scattering is discussed by several authors (33–36), but will not be given here.

For a foil (slab): $$f_{\text{th}} = 1 - \frac{z}{2}\left(0.923 + \ln\frac{1}{z}\right) \tag{10.11}$$

where $z = t/l$ (t = thickness of foil in cm).

For a sphere: $$f_{\text{th}} = 1 - \frac{9}{8} z \tag{10.12}$$

where $z = 2r/l$ (r = radius in cm).

A sample of powder or irregular pieces can be treated in terms of an equivalent sphere.

For a wire (cylinder): $$f_{\text{th}} = 1 - \frac{4}{3} z \tag{10.13}$$

where $z = r/l$ (r = radius in cm).

In these equations l is the absorption mean free path in the sample, defined by

$$l^{-1} = \sum N_i \sigma(\bar{v})_i \tag{10.14}$$

where N_i = density of ith nuclide (atoms. cm^{-3}); $= 6.10^{23}\delta\theta/A$ where the density δ depends on the physical form of the sample. For a powder, the apparent density must be taken;

$\sigma(\bar{v})_i$ = average absorption cross-section for ith nuclide. Assuming a Maxwellian distribution for $n(v)$, an approximate value for $\sigma(\bar{v})_i$ is given by

$$\sigma(\bar{v})_i = \sigma_{0i}\frac{\sqrt{\pi}}{2}\left(\frac{293.6}{T}\right)^{1/2} \tag{10.15}$$

(*cf.* section V, C, 1 of Chapter 3)

where σ_{0i} = 2200 m s^{-1} absorption cross section for ith nuclide (see Appendix 1, Table 1);

T = Maxwellian temperature.

In the case of 1 absorbing nuclide, equation (10.14) is simplified to $l^{-1} = N\sigma(\bar{v})$

In the case of one element containing different nuclides, the same simplification holds, where

$$\sigma(\bar{v}) = \bar{\sigma}_0\frac{\sqrt{\pi}}{2}\left(\frac{293.6}{T}\right)^{1/2},$$

$\bar{\sigma}_0$ being the average absorption cross section for the element, and N the atom density of the element.

Reynolds and Mullins (31) observed that when an equal amount of substance was irradiated as a solid or in solution, an enhancement of the reaction rate of 5% for 1.5 ml and of 12% for 30 ml solutions occurred. Hence:

$$\frac{R_{\text{solid}}}{R_{\text{solution}}} = f' = fa \tag{10.16}$$

The proportionality factor f' is the product of two components: the total absorption factor f, correcting for the finite dilution of the solid sample and a, which takes into account the enhancement in neutron density (a = 0.95 or 0.89 for respectively 1.5 ml and 30 ml solution).

This allows the calculation of the reaction rate at infinite dilution R, as follows:

$$R = \frac{R_{\text{solid}}}{f} = aR_{\text{solution}} \tag{10.17}$$

The effect of flux enhancement with increasing volume from intra-sample neutron moderation and reflection has also been studied by Johnson (37).

The effect of "flux hardening" (slower neutrons being absorbed more strongly than faster neutrons by nuclides whose cross-section follows the $1/v$-law) was shown to be neglibible in most activation analyses (38).

It is essential to realize that the factor f_{th} will be the same for all constituents of a sample, at least for nuclides having a σ_{abs} which follows the $1/v$-law up to the Cd cut-off energy: f_{th} can therefore be called a thermal self-shielding factor, applicable both to standards and samples.

(3) *Resonance absorption.* In order to calculate $f_e = I^{\text{eff}}/I$, according to Høgdahl, both the infinitely diluted resonance integral I and the effective resonance integral I^{eff} must be known for the nuclide of interest, or at least the ratio I^{eff}/I.

(a) Standards (comparators)

In the case of nuclides responsible for the main absorption and thus for the removal of the neutrons, f_e can be calculated, e.g. when dealing with pure materials. However, even approximate computations are laborious and lead not always to consistent results (39). Reasonably simple analytical expressions are given by Chernik and Vernon (40) for a single Breit-Wigner resonance i, without any correction for Doppler effect. The first equation is the "narrow resonance" (NR)-approximation, the second one the "narrow infinitely heavy absorber" ($NRIA$)-approximation.

$$(NR): \frac{I_i^{\text{eff}}}{I_i} = \left[1 + \frac{\beta}{\varepsilon+1} - \frac{\beta\Gamma_n}{\Gamma(\varepsilon+1)^2}\right]^{-1/2} \tag{10.18}$$

$$(NRIA): \frac{I_i^{\text{eff}}}{I_i} = \left(1 + \frac{\beta\Gamma_\gamma}{\varepsilon\Gamma}\right)^{-1/2} \tag{10.19}$$

$$\beta = \frac{\sigma_r(E_r)}{\sigma_p}; \quad \varepsilon = \frac{\delta S}{4N\sigma_p M} \tag{10.20}$$

where Γ_γ and Γ_n are the partial widths for gamma, respectively neutron emission and $\Gamma = \Gamma_\gamma + \Gamma_n$

δ, S and M: density, surface and mass of the lump

N: number of absorbing nuclides per cm³

$\sigma_r(E_r)$: total cross section at maximum of resonance (Table 10.3)

σ_p: potential scattering cross section $= 4\pi R_A^2$ (R_A = radius of the nucleus).

Whether to use the *NRIA* or *NR* approximation depends on whether the practical width $\Gamma[\sigma_r(E_r)/\sigma_p]^{1/2}$ is > or < than the maximum loss in a collision of a neutron with energy E_r (resonance energy) with a nuclide of atomic number A

$$\Delta E_{max} = E\left[1 - \left(\frac{A-1}{A+1}\right)^2\right].$$

For the *NRIA* approximation, $f_s = 1.1\ I_i^{eff}/I_i$ (30), whereas for the *NR* approximation $f_s = I_i^{eff}/I_i$. Some characteristic resonance parameters and material constants are given in Table 10.3.

If practically one resonance (I_1) determines I_{tot} (i.e. $\sum I_i \simeq I_1$) these calculations can lead to reasonably good results (e.g. In, Ag, Au).

If the contribution from many resonances must be taken into account, the calculation becomes too complicated (41) to be of practical interest in activation analysis.

In many cases it has no sense to have very "good" formulae, because they cannot be applied to practical problems due to the fact that accurate data are lacking (such as resonance integrals).

A very simple but different approach, which can therefore be recommended in many cases, has been described by Reynolds and Mullins (31) and is based upon data of self-shielding in cobalt (42). It was assumed that for any absorber of resonance neutrons an "effective thickness" t_{eff} exists, such that

$$t_{eff} = \frac{I_x N_x}{I_{Co} N_{Co}} t \qquad (10.21)$$

where I_x = resonance integral for element X

I_{Co} = resonance integral for cobalt (65 b)

N_x = atom density of element X (atoms/cm³) (in foil, powder ...)

N_{Co} = atom density of cobalt (in foil, powder ...)

t = thickness (cm) of foil, radius of wire, 2/3 of radius of sphere.

TABLE 10.3
Some characteristic Resonance Parameters and Material Constants (43)

Nuclide	θ(%)	E_r (eV)	$\sigma_r(E_r)$ (barn)	Γ_γ (eV)	Γ_n (eV)	Γ (eV)	I_{abs}, I_{act} * (total, $+ 1/v$)	δ(g. cm⁻³) elem.	δ(g. cm⁻³) massive	N (cm⁻³) × 10^{-22}
^{115}In	95.77	1.457	29,000	0.072	0.00304	0.075	3606 (= In)	7.28		3.82
^{197}Au	100	4.906	37,000	0.124	0.0156	0.1396				
		46.5	21				1558 (= Au)	19.3		5.9
		58.9	800							
^{109}Ag	48.65	5.20	34,000	0.140	0.0125	0.1525	1420 (^{109}Ag)	10.5		5.86
							760 (Ag)			
^{186}W	28.4	18.8	14,000	0.045	0.266	0.311	478 (^{186}W)	19.3		6.2
							355 (W)			
^{75}As	100	47	3100	0.296	0.039	0.335				
		92	653	0.269	0.016		40 (= As)	5.72		4.58
		253	1160	0.330	0.070					
^{59}Co	100	132	9700	0.416	4.78	5.2	77 (= Co)	8.71		8.9
		4220	225							
^{55}Mn	100	337	2830	0.6	21	21.6				
		1080	420	0.6	14	14.6	11.5 (= Mn)	7.42		8.14
		2360	702	0.6	340	340				
^{23}Na	100	2850	370	0.34	404.6	405	0.32 (= Na)			—
^{63}Cu	69.1	577	1550	0.4	1.26	1.30				
		2040	626	0.4	32.0	32.4	5.0 (= ^{63}Cu)	8.94		8.48
		5340	240	0.4	75.6	76.0	3.8 (Cu)			

* For a given resonance, I'_ξ can be calculated approximately from the other resonance parameters by the equation $I'_\xi = \pi\Gamma_\gamma\sigma_r(E_r)/2\,E_r$ (without $1/v$ – "tail").
The $1/v$ contribution = 0.44 σ_ξ ($I = I' + 0.44\ \sigma_\xi$).

By fitting empirical data on self-shielding of epicadmium neutrons in cobalt (42), the equation for the "attenuation factor" is:

$$f_e = -0.29 \log t_{eff} = -0.29 \log \frac{I_x N_x}{I_{Co} N_{Co}} t \qquad (10.22)$$

where $f_e = \varphi_e^{eff}/\varphi_e$, i.e. the average "resonance flux" in the sample divided by this value if the sample were absent. This is equivalent to the approach of Høgdahl, where $f_e = I^{eff}/I$. Indeed at high dilution $R_e = \varphi_e I$, thus:

$$R_e' = \varphi_e I^{eff} \text{ (Høgdahl)} = \varphi_e^{eff} I \text{ (Reynolds)}$$

hence:

$$f_e = R_e'/R_e = I^{eff}/I \quad \text{or} \quad \varphi_e^{eff}/\varphi_e$$

Obviously equation (10.22) is inaccurate for $t \to 0$ ($f_e \to 1$). Better results are obtained in this case by taking the effective cross section for the most important resonance as 1/10 the peak value and using equations (10.11) to (10.13). Some characteristic resonance parameters and material constants are given in Table 10.3.

The epithermal self-shielding factor can only be used to calculate the effect of absorption of resonance neutrons on the activity induced in the nuclides which are responsible for the main absorption of the neutrons, as is the case for resonance self-shielding in the standards.

The effect of resonance self-shielding in standards can be avoided by irradiation at a position where the flux is well thermalized. As will be shown further, the effect can be considered to be negligible if, for the nuclide of interest, $CR \geq 50$ (Figure 10.4). Another possibility is dilution of the standard in inert material. This is apparent from the experimental data reported by Eastwood *et. al.* (44), which are summarized in Table 10.4.

TABLE 10.4
Self shielding data for cobalt and dilute cobalt alloys (44)

Wire diameter (cm)	Cobalt content (mass %)	$f_{e(132eV)}$	f_{th}
0.127	0.104	1.00	1.00
0.127	0.976	0.95	0.99
0.00254	100	0.81	0.99
0.0254	100	0.42	0.94
0.0635	100	0.32	0.88

Some experimental and calculated values of f_{th} (equations (10.11)-(10.13)), f_e (equations (10.18), (10.19) or (10.22)), f (equation (10.10), assuming a cadmium ratio for gold = 2.85) and f' ($=0.95\,f$ in 1.5 ml solution or $0.89\,f$ in 30 ml solution to correct for flux enhancement, according to Reynolds and Mullins (31)) are given in Table 10.5.

Experimental data with powdered material were not checked by calculation, because the apparent density of the powder was not given.

(b) Samples

In activation analysis of samples the picture is usually more complicated. The effective resonance integral for the nuclide of interest (e.g. minor or trace constituent) is often less than the dilute integral (according to the terminology of Høgdahl), because of neutron absorption by the matrix or by nuclides which make up the main constituents of the sample. Usually $I^{eff} \approx I$, but in some cases where the bulk materials have absorption peaks which coincide with resonance peaks in the nuclide of interest, the effect of epithermal neutron absorption can be quite large. As an illustration Høgdahl considers I^{eff} for gold in samples of silver and cobalt (main resonance peaks, see Table 10.3).

Even if the gold content in silver is a few ppm, I^{eff} for gold will decrease rapidly with sample size, as appears from Table 10.6: I^{eff} for gold in a silver sphere of only 48 mg is ca. 85% lower than the dilute I, which can cause errors in activation analysis of 20–45%.

On the other hand, I^{eff} for gold at 4.91 eV is only a few percent lower than the dilute I in the case of 3% gold in a cobalt sphere of 1 g (resonance Co: 132 eV), because the resonances do not coincide.

It is very difficult to give general rules for calculating I^{eff} in the equation $R_e' = \varphi_e I^{eff}$ (30) for a specific nuclide in a particular sample, because the calculation will depend on the nuclide of interest and on the composition of the sample.

However, as already mentioned in the case of the standards, the effect of epithermal absorption can be made insignificant by diluting the sample with an inert material or, if this is not possible, by irradiating the sample in a proper reactor position, even if $I^{eff} \ll I$.

Assuming $0.5 < f_{th} \leq 1$ and $f_e \leq 1$, Høgdahl derives the following expression (30):

$$f - f_{th} \leq \frac{2}{CR} \qquad (10.23)$$

TABLE 10.5
Calculated and experimental values for f_{th}, f_e, f and f' for "pure substances" (standards) at an irradiation position $CR_{Au} = 2.85$

Material	Thickness or radius	Water volume	Active nuclide	f_{th}	f_e	f	f'	Ref. for f_e
Au foil	0.003 cm	1.5 ml	^{198}Au	0.96	0.35	—	—	Brose calc. (41)
					0.32	0.73	0.69	NRIA calc.
					0.43	0.77	0.74	Reynolds calc. (31)
				—	—	—	0.73	Reynolds exp. (31)
				—	0.35	—	—	Brose exp. (41)
In foil	0.013 cm	30 ml	^{116m}In	0.86	0.195	(0.57)	(0.51)	Bauman calc. (45)
					0.21	0.57	0.51	NRIA calc.
					0.30	0.56	0.50	Reynolds calc. (31)
				—	—	—	0.53	Reynolds exp. (31)
Ag foil	0.013 cm	1.5 ml	^{110}Ag	0.91	0.155	0.63	0.60	NRIA calc.
					0.33	0.70	0.66	Reynolds calc. (31)
				—	—	—	0.57	Reynolds exp. (31)
Au wire	0.0103 cm	—	^{198}Au	—	0.16	—	—	NRIA calc.
				—	0.245	—	—	Reynolds calc. (31)
				—	0.22	—	—	Mc Garry exp. (46)
Co wire	0.0255 cm	30 ml	^{60}Co	0.91	0.52	0.88	0.78	NRIA calc.
					0.47	0.89	0.79	Reynolds calc. (31)
				—	—	—	0.30	Reynolds exp. (31)
				0.90	0.34	(0.87)	(0.77)	Eastwood exp. (44)

i.e. if the CR of the nuclide of interest in the irradiation position used is ≥ 50, the accuracy of the analysis will be practically unaffected even by the existence of a serious absorption of epithermal neutrons by other constituents, as $f_{th} \approx f$ (or $f_e R_e/R \ll f_{th} R_{th}/R$). It can be useful to express the cadmium ratio for any nuclide in terms of the cadmium ratio for gold:

$$CR_x = 1 + (CR_{Au} - 1)\frac{I_{Au}\sigma_{0,x}}{I_x \sigma_{0,Au}}$$

or

$$CR_x = 1 + 15.6\,(CR_{Au} - 1)\frac{\sigma_{0,x}}{I_x} \qquad (10.24)$$

Measured and calculated values for resonance integrals are tabulated by Drake (47) (Appendix 2, Table 1).

Example: (i) Consider a silver sphere; ^{109}Ag has a prominent resonance peak at 5.1 eV. If copper is a minor constituent in the silver, the absorption of epithermal neutrons by the matrix will not seriously affect the specific activity of copper, even at an irradiation position where $CR_{Au} = 2.6$ (or $CR(^{63}\text{Cu}) = 32$, from equation (10.24)). This follows from equation (10.23) and can be seen in Table 10.6 (f(Cu) $\approx f_{th}$).

(ii) Consider again a silver sphere, containing gold as a minor constituent. The resonance peaks of ^{197}Au ($E_r = 4.91$ eV, ~97% of the total I) and of ^{109}Ag ($E_r = 5.1$ eV + many others) overlap con-

TABLE 10.6
Correction factors for neutron shielding of copper and gold in silver spheres (30)
(a) $CR_{Au} = 11{,}400$
(b) $CR_{Au} = 2.6$

Weight (mg)	Radius (mm)	f_{th} (Ag) = f_{th} (Ag,Au,Cu)	f_e(Cu) *	f(Cu) (a)	f(Cu) (b)	f_e(Au)	f(Au) (a)	f(Au) (b)
10.20	0.58	0.88	0.97	0.88	0.88	0.17	0.88	0.60
48.38	1.01	0.31	0.95	0.81	0.82	0.14	0.81	0.56
156.6	1.53	0.74	0.93	0.74	0.75	0.12	0.74	0.52
704.3	2.54	0.62	0.89	0.62	0.63	0.10	0.62	0.42

* It was not necessary to calculate f_e(Cu) (see text), as could be expected from equation (10.23) that f (Cu) $\simeq f_{th}$.

siderably and thermal neutron absorption by silver will have a large influence on the specific activity of ^{198}Au. However, if the irradiation is done at a place where CR_{Au} is sufficiently high (e.g. 11,400, see Table 10.6) the effect is negligible and again $f(\mathrm{Au}) \approx f_{th}(\mathrm{Au}) = f_{th}(\mathrm{Ag})$.

If the sample cannot be diluted and/or if CR for the nuclide of interest is not ≥ 50, f_e must be calculated. There are two possibilities:

(i) No overlapping of resonances occurs.

(ii) The main absorption resonances in the nuclide of interest overlap practically completely with main resonances in the nuclides which make up the main constituents in the sample.

Examples: (i) copper in silver.

Calculations are given by Høgdahl (23,30), but will not be repeated here, as the f_e value does not influence f(Cu), see above.

(ii): gold in silver.

f_e was calculated as follows. As ^{197}Au has its main resonance at approximately the same neutron energy where ^{109}Ag also has a prominent peak, it is reasonable to assume that I_1^{eff}(Au) will decrease at the same rate as I_1^{eff}(Ag), i.e.

$$\left(\frac{I_1^{eff}}{I_1}\right)_{Au} \approx \left(\frac{I_1^{eff}}{I_1}\right)_{Ag} \quad \text{Further} \quad \left(\frac{I_1^{eff}}{I_1}\right)_{Au} \approx \left(\frac{I_{tot}^{eff}}{I_{tot}}\right)_{Au} \tag{10.25}$$

$(I_1^{eff}/I_1)_{Ag}$ can be calculated according to Chernick and Vernon (40) if the resonance parameters are known (see Table 10.3; $\sigma_p = 4.7$ b). As $\Gamma[\sigma_r(E_r)/\sigma_p]^{1/2} = 0.1525\ (34{,}000/4.7)^{1/2} = 12.95$ eV; since this is more than ΔE_{max} for neutrons of 5.1 eV, the NRIA approximation must be followed, and 10% added to the calculated value of I_1^{eff}/I_1. By putting the approximate resonance parameters and the value $0.4865 \times 5.86 \times 10^{22}$ for the number of ^{109}Ag nuclides/cm^3 (N) into this equation, one gets

$$(I_1^{eff}/I_1)_{Ag} = (1 + 1180\, r)^{-1/2} \tag{10.26}$$

where r = radius of the sphere in cm (S/M for a sphere $= 4\pi r^2/\frac{4}{3}\pi r^3\delta = 3/\delta r$). Only approximate calculations for I^{eff} (the total resonance integral) are possible as reliable data for all the resonance parameters are lacking: consequently differences of 20–40% for I_{eff} between two extreme values are found.

However, the difference between the corresponding f-values is only 3.5% even in an irradiation position where $CR_{Au} = 2.6$. Calculated values for f_e are given in Table 10.6. f_{th} was calculated from equations (10.12) and (10.14) assuming an alloy containing the average between 94% Ag, 1% Au and 5% of elements with zero absorption cross section, and 98% Ag, 1% Au and 1% Cu ($l = 0.0187\sqrt{T}$ cm, where $T = 395$°K for $CR_{Au} = 2.6$, and $T = 340$°K for $CR_{Au} = 11{,}400$). f was calculated from equation (10.10). The copper content of the silver spheres can be calculated from:

$$\frac{A_x}{1.025\, A_s} = \frac{w_x}{w_s} f_{Cu} \tag{10.27}$$

where w_s is the weight of the copper standard (30 mg pellets). The factor 1.025 corrects for self-shielding in the copper standard ($f \approx 0.97$).

The gold content can be calculated from

$$\frac{A_x}{0.97\, A_s} = \frac{w_x}{w_s} f_{Au} \tag{10.28}$$

where w_s is the weight of the gold standard (10.50 and 75 μg gold in 0.75 ml solution); the factor 0.97 corrects for thermal enhancement in the gold standard solutions. Good agreement was found between results of activation analysis and classical analysis,

nl. Cu: act. anal. 1.03%; classical analysis 1.07%
Au: act. anal. 1.05%; classical analysis 1.03%

From Table 10.6 it is apparent that even for silver spheres, weighing only 10 mg, errors of 12% for copper and 12–40% for gold (depending on the irradiation position) can be made, if no corrections are made.

Because the general complexity of the problem of calculating the effects of neutron absorption often prohibits an accurate theoretical treatment, an analysis should, if possible, be carried out by a method which either eliminates or experimentally determines the absorption effects. The above discussion is, however, useful to design the analysis so as to minimize errors.

Remark: In the case of absorption of a directed flux of monoenergetic neutrons (e.g. 14 MeV neutrons from a small accelerator) the problem is simpler. The attenuation process can, indeed, be expressed as a simple exponential law. It is, however, important to use the appropriate attenuation coefficients, nl. the cross sections for effective removal of

14 MeV neut... , as indicated in Appendix 4, Table 5. The problem is illustrated by an example, given in Chapter 7, section II, A.

(c) Corrections

(1) *Choice of neutron spectrum.* If the self-shielding is due to resonance absorption only, the effect can be made negligible by irradiating in a well thermalized neutron spectrum (e.g. Figure 10.4). If a thermal column is used, where the cadmium ratio for ^{121}Sb or ^{123}Sb is large (>50), antimony spheres weighing up to 100 mg can be irradiated without introducing any errors due to absorption effects. At an irradiation position where $CR_{Au} = 2.6$ (CR ^{121}Sb = 2.08; CR ^{123}Sb ≒

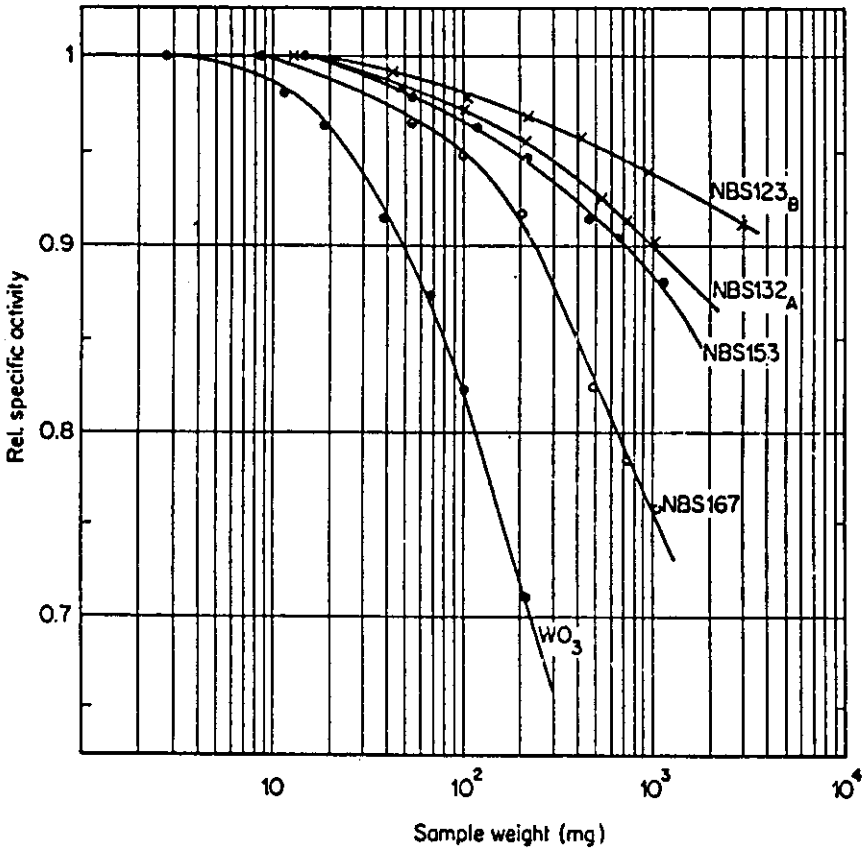

Fig. 10.7. Influence of sample size on the neutron self-shielding (48).

1.5) errors of 40% can occur with an antimony standard of 100 r ...3).

(2) *Dilution method.* If the self-shielding is due to resonance or thermal absorption, the effect can often be eliminated by using sufficiently small samples. Some practical data for the influence of sample size on the neutron shielding for different NBS steels, containing cobalt and tungsten, are given in Figure 10.7 (48). Some elements have, however, such large absorption cross sections, that f will be significantly smaller than unity, even for samples of less than 10 mg (Ag, Au, Rh, Ir, In, Hg, Cd, . . .). If such an element is the matrix material, the high σ_{abs} value can be compensated for by a sufficiently low value of N_f or N (atoms/cm^3) (see for instance equations (10.11)–(10.13) in the case of thermal absorption and equations (10.18)–(10.20) in the case of resonance absorption), in other words, by diluting them with materials which have low absorption cross sections (water, graphite, lead powder, sugar, MgO, CaO, Al_2O_3, SiO_2 . . .). If large volumes of water are used for dilution, flux enhancement must be taken into account (32,37). The effect of diluting Sb_2O_3 with graphite or lead is represented in Figure 10.8 ($CR_{Au} = 5.5$ at the irradiation position used).

For a total weight of 1 g, Sb_2O_3 must be diluted with at least 50 times its own weight of graphite to obtain a constant specific activity (22).

From Table 10.4 it appears that even for thick wires of a dilute Co–Al alloy, thermal and resonance self-absorption are negligible. If such an element is used as a standard, it is normally irradiated as a dilute solution or a known quantity of that solution can be spotted on a filter paper and dried (49).

Remark: The dilution method can eliminate self-absorption effects, but it is still possible that samples and standards are not exposed to the same external neutron flux. The difficulty of an inhomogeneous flux can be overcome by irradiating the targets one after another and using a small flux monitor attached to a fixed position in the irradiation can or rabbit. In some cases an internal standard can be used (see further), not only for reactor, but also for 14 MeV neutron irradiation, where the flux inhomogeneity can be an important source of error.

(3) *Standard addition method.* It is not always possible to eliminate self-absorption effects, particularly if the matrix has a high absorption cross section. A typical example is the determination of impurities in cobalt metal by Speecke and Maes (40). It is then simpler to design the

cadmium ratio for the isotope used in the determination is large (>50). Then:

$$\frac{A_t}{A_t^*} = \frac{ax + c}{bx}\alpha \tag{10.30}$$

where A_t and A_t^* are the measured activities of a suitable radionuclide of the element under investigation, at time t, in the sample containing $ax + c$ and bx mg of the element respectively; x is the concentration of the element, which can be calculated as a, b and c are known and as A_t, A_t^* and α (from equation 10.29) are measured. Note that the two samples need not be irradiated in the same can or even at the same time, and that the correction factor α corrects for both inhomogeneities of the neutron flux and for a different thermal neutron absorption in the two samples.

If the CR for the nuclide of interest is not >50, some specific requirements must be added (23). Indeed, by using equations of the same form as equation (10.9) one gets:

$$\frac{A_t(\mathrm{St})}{A_t^*(\mathrm{St})} = \frac{a}{b}\left(\frac{\sigma_{\mathrm{reactor}}^{\mathrm{eff}}}{\sigma_{\mathrm{reactor}}^{*\mathrm{eff}}}\right)_{\mathrm{St}}\frac{\bar{n}_{\mathrm{th}}}{\bar{n}_{\mathrm{th}}^*} \tag{10.31}$$

and

$$\frac{A_t}{A_t^*} = \frac{ax + c}{bx}\frac{\sigma_{\mathrm{reactor}}^{\mathrm{eff}}}{\sigma_{\mathrm{reactor}}^{*\mathrm{eff}}}\frac{\bar{n}_{\mathrm{th}}}{\bar{n}_{\mathrm{th}}^*} \tag{10.32}$$

Therefore, the condition which must be fulfilled is:

$$\left(\frac{\sigma_{\mathrm{reactor}}^{\mathrm{eff}}}{\sigma_{\mathrm{reactor}}^{*\mathrm{eff}}}\right)_{\mathrm{St}} = \frac{\sigma_{\mathrm{reactor}}^{\mathrm{eff}}}{\sigma_{\mathrm{reactor}}^{*\mathrm{eff}}} \tag{10.33}$$

From equation (10.8) and the definition of the cadmium ratio follows, that this condition will be fulfilled (1°) if the absorption effect for thermal neutrons is the same:

$\bar{n}_{\mathrm{th}}/n_{\mathrm{th}} = \bar{n}_{\mathrm{th}}^*/n_{\mathrm{th}}^*$, i.e. that the samples are approximately equal in weight and in geometrical shape; (2°) if the CR for the two irradiation positions is the same for the two samples: $\varphi_e/n_{\mathrm{th}} = \varphi_e^*/n_{\mathrm{th}}^*$, i.e. the CR does not change rapidly with the space coordinates if the samples are irradiated simultaneously and (3°) if $I^{\mathrm{eff}} = I^{*\mathrm{eff}}$ and $I^{\mathrm{eff}}(\mathrm{St}) = I^{*\mathrm{eff}}(\mathrm{St})$, i.e. that the isotope of the element of interest, of which the induced activity is used in the determination, has no large resonance peaks, so that its addition (c) does not change I^{eff} or $I^{\mathrm{eff}}(\mathrm{St})$ (53).

If this nuclide has peaks which overlap resonance peaks in the

nuclide used as internal standard or overlap resonance peaks in the nuclides which make up the main constituents in the sample, restrictions must be set to the amount c of the element added (see above: hypothetical example of determining gold in iron). In the above references, the activities of tungsten, vanadium and manganese and of the internal standards were counted in steel without chemical separation. In the following example, the addition method is used together with the internal standard method for the determination of traces of iridium in ruthenium (54). Six ruthenium samples of 5 mg, containing ca. 0.04% of Ir, were irradiated in solution; to three samples 2.5 μg of Ir (i.e. 0.050%) was added prior to activation. After irradiation, the ruthenium matrix was distilled and its activity used as an internal standard. The iridium activity could be measured in the residue without further chemical separations. Some data are given in Table 10.7.

TABLE 10.7
Determination of Ir in commercial Ru by the addition method and using the ^{103}Ru activity as an internal standard

% Ir added	Height 317 KeV photopeak (^{103}Ir)	Height 498 KeV photopeak (^{103}Ru in distillate)	Height 317 KeV (normalized)
0	11,500	12,650 (=1)	11,500
0	9,150	12,260	9,440
0	11,070	13,750	10,185
0.050	20,020	11,613	22,005
0.050	25,350	13,200	24,295
0.050	16,300	8,070	25,550

Another example (55) where the addition method and the internal standard method are used together is the determination of gold (^{198}Au measured, 411 KeV photopeak) in platinum after separation of the gold activity from the sample, using ^{199}Au (daughter of ^{199}Pt, photopeaks at 158 and 208 KeV) as an internal standard. Counting is carried out using a lead absorber to reduce pile up of the ^{198}Au activity.

The ratio ^{198}Au/^{199}Au is directly proportional to the gold content in platinum and is independent from flux inhomogeneities, from

absorption ... ...ts and even from different weight, different chemical yield and different counting time (as $T_{1/2}(^{198}\text{Au}) \approx T_{1/2}(^{199}\text{Au})$). Some data are shown in Table 10.8.

TABLE 10.8
Measured net activities of ^{198}Au (411 KeV) and ^{199}Au (208 KeV)

Sample	mg	Counting time	208 KeV (net)	411 KeV (net)	411 KeV / 208 KeV
Pt 1	54	30 m	160,240	1,940	0.01123
Pt 1	100	30 m	292,052	3,446	0.01179
Pt 1 + 1.14 ppm Au	100	30 m	279,088	7,316	0.02621
Pt 2	100	3 m	23,249	9,754	0.4195
Pt 2	100	3 m	32,016	13,362	0.4174
Pt 2	100	3 m	32,794	14,738	0.4494
Pt 3	100	3 m	32,222	11,649	0.3615
Pt 3	100	3 m	20,598	7,367	0.3577
Pt 3	100	3 m	31,138	11,520	0.3700

From the sample with addition one finds that for 1 ppm of gold the ratio 411 KeV/208 KeV is 0.01287, hence the gold content for samples 1, 2 and 3 can be calculated to be 0.90, 32.8 and 27.7 ppm respectively.

De Soete, De Neve and Hoste (56) described a γ-spectrometric determination of As in Ge (^{76}As measured at 1.21 MeV), after chemical separation of As_2S_3 from the Ge-oxalate complex, using ^{77}As (daughter of ^{77}Ge measured at 0.246 MeV) as an internal standard. The ratio ^{76}As/^{77}As can better be determined by β-spectrometry, using a plastic scintillator (Figure 6.19). The maximum β-energy for ^{77}As is 0.700 MeV, for ^{76}As 2.98 MeV.

Remark: The addition method, the internal standard method and the dilution method all suffer from two disadvantages:

(1) a really homogeneous mixture must be obtained for the method to be valid (ideal situation: irradiation in solution);

(2) the manipulation of the samples prior to activation introduces the possibility of contaminating the samples. This is particularly dangerous in the case of trace analysis for common elements (Cu, Zn, As, ...). In the case of minor constituent analysis (V, W, ... in steel) or trace analysis for rarer elements (Ir in Ru) this aspect becomes less important.

The two disadvantages mentioned disappear if the specific activity of the element under investigation can be found from standard samples of known content. For trace analysis this is however a difficult problem. Wood (57) describes the determination of silicon in iron and steel with 14 MeV neutrons, using ^{56}Mn (formed by (n, p) reaction on ^{56}Fe) as an internal standard. No silicon is added to determine the specific activity of ^{28}Al, but a series of NBS and BCS samples is used to construct a calibration curve. The ratio ^{28}Al/^{56}Mn is directly proportional to the content of silicon and is independent from the flux. Again, the internal standard is used to correct as well for neutron flux inhomogeneity, as for self-absorption. Routine analyses of silicon (~3%) in magnetic steel, with a standard deviation of ca. 1% for a single determination, have recently been described. The net ^{28}Al and ^{56}Mn activities were counted using two single-channel analyzers (58).

(5) *Extrapolation method.* The effect of self shielding is readily demonstrated by irradiating a series of samples of varying weight and containing the element of interest. After calculating the concentration of the element, without correcting for any absorption effects, the results are plotted versus sample weight. By extrapolation to zero weight one obtains the content corrected for self-absorption. This method (59) does not require a manipulation of the samples prior to irradiation. It is however obvious that the method requires a homogeneous neutron flux over the samples and the standards, because it can only correct for self-absorption. This was also the case for all the methods above, with the exception of the internal standard method.

The method must be used with precaution, as was pointed out by Høgdahl (23). In Figure 10.9 the gold content in silver spheres of different weight is plotted against the sample weight, without any correction for neutron absorption: (a) after irradiation in a "thermal column" (CR_{Au} = 11,400) and (b) after irradiation in a "fast column" (CR_{Au} = 2.6). The values (c) were determined after correction (Table 10.6). Extrapolation of curve (a) can easily introduce errors of ca. 5% if data of samples down to 10 mg are available, and errors of ca. 20% for samples down to 150 mg.

In the case of curve (b) the extrapolation method is quite inapplicable, because errors of ca. 40% are introduced, even if samples weighing

only 10 mg are analyzed. It is practically impossible to analyze samples so small that an accurate extrapolation can be performed.

Therefore, if the bulk part of the matrix has large resonance absorption peaks which overlap those of the isotope under investigation, the method can only be used if the irradiations are carried out at a place in the reactor where the cadmium ratio is large (>50). In this case the contribution to the total induced activity due to epithermal neutrons is small and the method must be combined with the first one (choice of neutron spectrum). But even then the effect of thermal neutrons can sometimes make it difficult to use this method, as very small samples (e.g. 10 mg) must be analyzed.

(6) *Other methods.* (a) *Neutron filters.* If matrices with a high absorp-

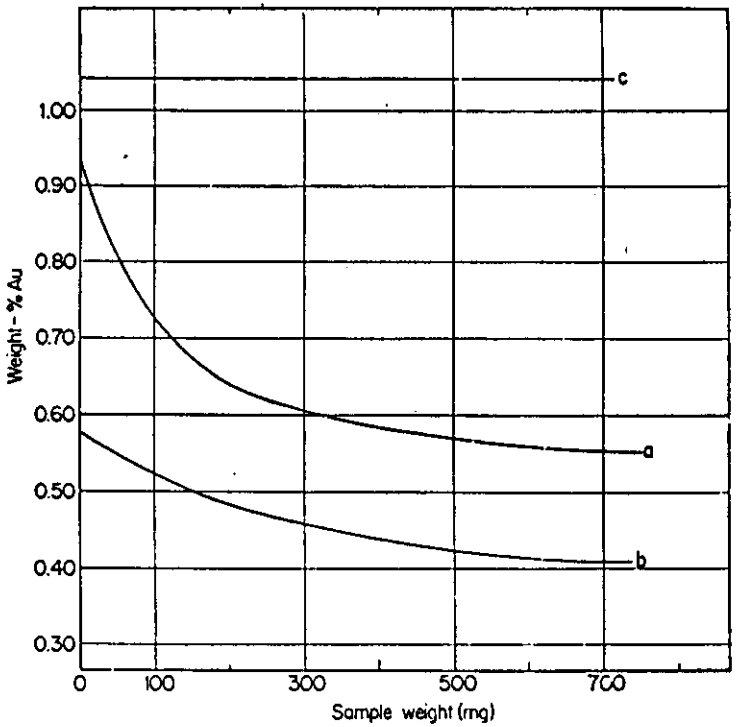

Fig. 10.9. Concentration of Au in Ag-spheres. (a) without correcting for absorption effects ($CR = 11{,}400$), (b) without correcting for absorption effects ($CR = 2.6$), (c) after correction for absorption effects (see Table 10.6) (23) (30).

tion cross section are to be analyzed, as for instance cadmium, it is also possible to avoid neutron shielding differences between the samples and the standards by irradiating them in a sufficiently thick box or foil of the matrix element (Cd in this example).

This method was followed by Baumgärtner (60) for the determination of chlorine in cadmium. The impurities will obviously only be activated by neutrons which are not absorbed by the cadmium foil, hence the sensitivity will decrease. However, the sensitivity is in many cases sufficiently high, particularly if the activation is carried out in the reactor core, even in the unfavourable case of resonance absorption of thermal neutrons. Care must be taken to use no packing material, such as polythene, after the "neutron filter", to avoid secondary moderation. This method can also be used in the analysis of epithermal resonance absorbers, such as gold, silver and indium.

(b) *Separation prior to activation.* In some cases it is possible to separate the matrix before irradiation. Ördögh *et al.* (61) removed the bulk of uranium from their samples by a specific paper chromatographic method prior to activation: a nitric acid–ether mixture removes the uranium (ca. 100 mg) which leaves the paper, while other cations (Ag, Cr, Co, Fe, P, Cd) remain at the starting position. This procedure eliminates also the formation of high activities due to the production of ^{239}Np and of various fission products from uranium. These could give rise to primary interference (see next section). Copper and molybdenum contamination was, however, observed.

If elements like Mo, Ru, Te ... must be determined in uranium, the matrix must be completely removed to avoid primary interference (see further). A complete removal is, however, practically impossible without losses of the elements to be determined. For that reason, Pauly *et al.* (62) used a combination of isotope dilution (to determine the chemical yield of the preseparation) and activation analysis. As the analysis is by isotope dilution, the separation does not need to be quantitative and can be carried out so as to minimize the blank correction.

Another approach has been described by Mark *et al.* (63) for the determination of gold in sea water. The noble metal is deposited on a cathode of pyrolytic graphite; the lower end of the cathode is then cut off and irradiated. This procedure eliminated the formation of high ^{24}Na + ^{38}Cl activities, but introduced also the possibility of contaminating the samples from reagents, electrodes, etc. Correction can

however eas. _ ..e performed by a blank determination. Other examples are given in Chapter 7, section I, H.

(C) Interfering Nuclear Reactions

Apart from self shielding for thermal or resonance neutrons in the samples or in the comparators and failure to detect flux gradients at the irradiation position, other nuclear sources of error must be considered, e.g. interference from primary and second order reactions.

1. *Primary Reactions*

(a) (n, p) *and* (n, α) *reactions.* As an (n, p) reaction on element $Z + 1$ or an (n, α) reaction on element $Z + 2$ can give the same reaction product as an (n, γ) reaction on element Z, it is obvious that the presence of elements $Z + 1$ or $Z + 2$ can interfere with the determination of element Z. The same reactions induced in the next adjoining elements may also interfere if they produce radionuclides which decay through positron emission or electron capture to the activation products of interest.

The interference will obviously be more or less serious, depending on the relative concentrations of the target nuclides in the sample, on the ratio fast/thermal flux and on the ratio of the cross sections involved. Fortunately, the cross sections for (n, p) and (n, α) reactions are generally quite low compared to the (n, γ) cross sections, so that these reactions normally (not always) cause serious interference only in the presence of macro-quantities of the interfering elements (i.e. the interfering element is the matrix, or the element to be determined is present in extremely low concentration and the interfering element is a minor constituent). This interference will, of course, be less important or even negligible if the irradiation is carried out in a well thermalized neutron spectrum.

The importance of a primary interference can be estimated, if the ratio thermal/fast flux for the irradiation position and the values σ_0(n, γ) and $\bar{\sigma}$(n, p) . . . for the nuclides concerned are known; σ_0(n, γ) is given in Appendix 1,* whereas $\bar{\sigma}$(n, p), $\bar{\sigma}$(n, α) for a number of nuclides is given in Appendix 3. For other cases, estimated $\bar{\sigma}$-values by

*Actually the value $\sigma_{reactor} = g\sigma_0 + (\varphi_r I/\varphi_{th})$ must be used in the calculations (see section I of this chapter).

Roy and Hawton (64) can be used. The calculation will be given for the determination of copper in zinc from measurements of the ^{64}Cu activity, for an irradiation position where $\varphi_{th} = 4 \times 10^{11}$ and $\bar{\varphi} = 2.17 \times 10^{10}$ n cm^{-2} s^{-1} (*cf.* Chapter 3, section VI, B).

Reaction: ^{63}Cu (n, γ)^{64}Cu, $\theta = 0.691$, σ_0(n, γ) = 4.3 b, $\varphi_{th} = 4 \times 10^{11}$, $A = 63.54$ (at. weight).

Interfering reaction: ^{64}Zn(n, p)^{64}Cu, $\theta' = 0.489$, $\bar{\sigma}$(n, p) = 39 mb, $\bar{\varphi} = 2.17 \times 10^{10}$, $A' = 65.17$.

The ratio of the ^{64}Cu activities, produced respectively from 1 g of natural zinc and 1 g of natural copper is given by (*cf.* equation 10.1)

$$\frac{A\theta'\bar{\varphi}\bar{\sigma}(\mathrm{n,p})}{A'\theta\varphi_{th}\sigma(\mathrm{n},\gamma)} = 3.50 \times 10^{-4} \qquad (10.34)$$

(see also Chapter 3, section V, C, 3b (6)).

This means that an apparent copper content of 350 ppm will be found in copper-free zinc. Mellish *et al.* (65) measured an interference equivalent to ca. 700 ppm after irradiation in the centre of BEPO. Irradiation at the edge of the reactor reduced this error to ca. 1 ppm. Gijbels (54) found in rhodium an apparent ruthenium content of 17 ppm, due to the reaction ^{103}Rh (n, p)^{103}Ru ($\bar{\sigma} = 0.11$ mb), by irradiating the samples in the isotope train of the BR–1 reactor (Mol, Belgium). The cross section for the reaction ^{102}Ru(n, γ)^{103}Ru is 1.44 b.

The nuclear reaction ^{56}Fe(n, p)^{56}Mn ($\bar{\sigma} = 0.93$ mb) will interfere with the determination of manganese in iron. Bouten (53) found that the ^{56}Mn/^{59}Fe activity ratio was 13, 5 and 0 for a cadmium ratio (measured with gold) of 5, 40 and 150 respectively. Hence, the irradiations were carried out in the reflector of the BR–1 reactor, to eliminate spurious ^{56}Mn activities.

The determination of vanadium in high-alloy steels containing chromium can be disturbed by the reaction ^{52}Cr(n, p)^{52}V. Hoste (48) calculated an error of 1% for a chromium/vanadium ratio of 1000/1, if irradiations were carried out near the reflector of BR–1 ($CR_{Au} = 280$; $\varphi_{th} = 10^{10}$ n cm^{-2} s^{-1}). This is normally negligible. In less favourable conditions, however, the error can become quite important. In activation analysis with a cyclotron, where neutrons are produced with 26 MeV deuterons on a beryllium target and thermalized in a 20 cm paraffin block, a chromium/vanadium ratio of 1000/1 would give rise to a 220% error.

In a similar way, the reaction ^{27}Al(n, α)^{24}Na ($\bar{\sigma} = 3.1$ mb) gives a

spurious sodium activity equivalent to 81 ppm in the determination of sodium ($\sigma_0 = 0.54$ b) in aluminium (66).

For a thermal to fast flux ratio of 7.7, apparent concentrations for zinc and gallium in GeO_2 of 11.2 and 0.36 ppm respectively were found from the reactions $^{72}Ge(n, \alpha)^{69m}Zn$ and $^{72}Ge(n, p)^{72}Ga$. Consequently it is impossible to determine directly Zn and Ga in high purity germanium, if a completely thermalized neutron flux with sufficient intensity is not available. Separation of the bulk of the germanium prior to activation is then required (67).

Due to the interfering reaction $^{110}Cd(n, p)^{110m}Ag$, silver cannot directly be determined in CdS. Lux (68) used therefore an electrolytic separation before irradiation. The increased probability of disturbing (n, p) or (n, α) reactions by fast neutrons, if activation is carried out in high neutron fluxes ($1\text{–}3 \times 10^{14}$ n cm^{-2} s^{-1}) is discussed by Maslov (69) for a number of cases: ^{24}Na in Mg and Al, ^{42}K in Sc, ^{56}Mn in Fe and Co, ^{64}Cu in Zn, ^{72}Ga in Ge, ^{59}Fe in Co and Ni, ^{69m}Zn in Ge, ^{110m}Ag in Cd, ^{45}Ca in Ti, and ^{32}P in S and Cl. (See also Chapter 7, section I, H).

The above considerations can also be applied to the inverse problem. For the experimental determination of an average cross section in a fission neutron spectrum, $\bar{\sigma}(n, p)$, $\bar{\sigma}(n, \alpha)$, the element Z concerned must be free from elements Z–1 or Z–2, e.g. aluminium must be free from sodium to determine the $\bar{\sigma}$ of $^{27}Al(n, \alpha)^{24}Na$. The problem can, however, partly be solved by irradiating the samples under cadmium, to avoid thermal activation by the reaction $^{23}Na(n, \gamma)^{24}Na$. Epithermal activation is then still possible, of course.

Sometimes the "interfering reaction" is used instead of the thermal neutron reaction, if its sensitivity is better and/or the radionuclide formed is more easily detected. A typical example is the determination of sulfur by the sensitive fast neutron reaction $^{32}S(n, p)^{32}P$ (^{32}S: $\theta = 95.0\%$; $\bar{\sigma}(n, p) = 60$ mb; ^{32}P: $T_{1/2} = 14.3$ d) instead of $^{34}S(n, \gamma)^{35}S$ (^{34}S: $\theta = 4.22\%$; $\sigma_0 = 260$ mb; ^{35}S: $T_{1/2} = 87$ d). Moreover, ^{35}S is a much weaker β-emitter (0.167 MeV) than ^{32}P (1.701 MeV).

Similarly, ^{48}Sc and ^{49}Sc are formed by (n, p) reactions on ^{48}Ti and ^{49}Ti and have half-lives of 44 h and 57 m respectively, whereas the half-life of ^{51}Ti, formed by (n, γ) reaction on ^{50}Ti, is 5.8 m only. The latter isotope cannot be used for analysis if one must wait some time after the end of the neutron irradiation. See also Chapter 7, section IV, B.

In fast neutron activation, interfering reactions are more important, as the cross sections for the reactions concerned are of the same order of magnitude. Consequently serious interference can be caused by the presence of even small amounts of another nuclide (other trace impurity).

Example: the presence of fluorine in a sample will interfere with the determination of oxygen by the reaction $^{16}O(n, p)^{16}N$ ($\sigma_{14\,MeV} = 40$ mb; $\theta = 99.758\%$), due to the formation of the same radionuclide by the reaction $^{19}F(n, \alpha)^{16}N$ ($\sigma_{14\,MeV} = 57$ mb; $\theta = 100\%$). The cross sections are of the same order of magnitude. Correction is possible if the fluorine concentration is determined by an independent reaction: $^{19}F(n, p)^{19}O$ ($\sigma_{14\,MeV} = 135$ mb, other references: 15 mb). ^{19}O is longer lived than ^{16}N (29.4 s against 7.4 s) and can be determined after the decay of ^{16}N.

It is worthwhile to note here, that in 14 MeV neutron activation analysis of short-lived isotopes, interference from another element is often possible, even if another radionuclide is formed other than in the reaction of interest. In many cases short-lived radionuclides emit high energy β's or γ's, making a specific determination difficult or even impossible. High intensities of β- or γ-rays of lower energy can interfere also by pile up in the detector and (or) counting equipment. The presence of boron interferes with the determination of oxygen (^{16}N: $\gamma = 6.13$ MeV + others; $T_{1/2} = 7.4$ s) by the reaction $^{11}B(n, p)^{11}Be$ (^{11}B: $\theta = 80.93\%$; $\sigma_{14\,MeV} = 3.2$ mb; $T_{1/2} = 13.6$ s) due to high energy β-rays (11.5 and 9.3 MeV); errors of 100% are reported for a ratio boron/oxygen = 10/1 to 40/1 depending on experimental conditions. Similarly, the determination of oxygen in selenium is disturbed by the 5.4 and 6 MeV β-rays of ^{80}As, formed by the reaction, $^{80}Se(n, p)^{80}As$ (^{80}Se: $\theta = 49.82\%$, $\sigma_{14\,MeV} \simeq 13$ mb; $T_{1/2} = 15$ s). If the interfering radionuclide has a half-life $\gg$7.4 s, correction is possible by two subsequent countings. The difference is a measure for the ^{16}N activity.

(b) (n, f) reactions

Another primary interference reaction in thermal neutron activation is the presence of fissionable material. Even if only a small amount of such a nuclide (^{235}U for instance) is present in a sample, it can cause significant and often unexpected errors in the determination of many elements in certain regions of the periodic table. Dams (70) found

serious interferences from traces of uranium in the determination of very low concentrations of molybdenum and tellurium in $ZnSO_4$ solutions for industrial zinc electrolysis. ^{235}U traces are also found in HF, which is a by product of uranium diffusion plants. For a given U content in the sample, the interference depends on the fission yield for the radionuclide of interest and on the activation cross section and isotopic abundance of the "corresponding" stable nuclide. Very unfavourable cases are Mo, Te and Ce for instance. The interference can be estimated in the following way. Assuming that 1 g of natural uranium is present, the activity for a given isotope i from fission can be calculated from

$$A_i(\mathrm{n,f}) = y_i \sigma(\mathrm{n,f}) \varphi_{\mathrm{th}} N_A S_i / A_u \qquad (10.35)$$

where $\sigma(\mathrm{n,f})$ = the cross section of natural uranium for fission = 4.18 b
A_u = atomic weight of natural uranium = 238.03
N_A = Avogadro's number
$S_i = 1 - \exp(-\lambda_i t_b)$ where λ_i = disintegration constant for the isotope i
y_i = total fission yield for the isotope i.

For the (n, γ) reaction, equation (10.1) must be used. For 1 g of the element x, one calculates

$$A_i(\mathrm{n},\gamma) = \sigma(\mathrm{n},\gamma) \theta \varphi_{\mathrm{th}} N_A S_i / A_x \qquad (10.36)$$

The ratio $A_i(\mathrm{n,f})/A_i(\mathrm{n},\gamma)$ gives the interference:

$$\text{interference} = \frac{A_i(\mathrm{n,f})}{A_i(\mathrm{n},\gamma)} = \frac{4.18\, y_i A_x}{238.03\, \theta \sigma(\mathrm{n},\gamma)} \qquad (10.37)$$

Examples: ^{141}Ce (y = 0.06; θ = 0.88; σ(n, γ) = 0.31 b), interf. = 0.54
^{143}Ce (y = 0.057; θ = 0.11; σ(n, γ) = 1 b), interf. = 1.26
^{147}Nd (y = 0.027; θ = 0.17; σ(n, γ) = 2 b), interf. = 0.20
^{153}Sm (y = 0.0015; θ = 0.26; σ(n, γ) = 140 b), interf. = 0.0001
^{99}Mo (y = 0.061; θ = 0.24; σ(n, γ) = 0.5 b), interf. = 0.85.

From these data it follows that trace analysis for light rare earth elements (maximum fission yield) in minerals by neutron activation analysis will be practically impossible, if uranium is present in the same concentration range. For the heavy members of the group (lower fission yield) the situation is less unfavourable (71).

In practice, the importance of this interference for a given isotope can be estimated by determining the uranium content of the sample from the ^{239}Np activity, and then determining (or at least calculating) the activity of the radionuclide of interest, which should be formed from that amount of uranium in the same experimental conditions. If the interference is too high, it can even be better to separate uranium from the sample prior to activation (see above).

A special case of primary interference can occur during the determination of bismuth in lead through the reaction $^{209}Bi(n,\gamma)^{210}Bi$. The ^{210}Bi activity ($T_{1/2}$ = 4.99 d) can also be present as a member of the ^{238}U series. Consequently, the mass-activity proportionality is not maintained. This error can be estimated by determining the activity of ^{210}Bi (or its daughter ^{210}Po) in lead without neutron activation (72).

2. *Secondary Reactions*

Secondary reactions are induced by γ-rays or charged particles available from (n, γ) or (n, p) and (n, α) reactions. These reactions are seldom significant in reactor irradiations because the photons and charged particles, created by reactor neutrons, have either too low an energy or too low an intensity to be significant (73). Cuypers (74) discusses the formation of ^{13}N in polyethylene by 14 MeV neutron irradiation. By collision of 14 MeV neutrons with hydrogen atoms in the sample, high-energy protons are formed, which interact with the carbon and give the $^{13}C(p,n)^{13}N$ reaction (Q=2.26 MeV; $T_{1/2}$=10 m). The same reaction limits the determination of nitrogen in hydrocarbons by the reaction $^{14}N(n,2n)^{13}N$ to concentrations greater than 0.1% (75).

A theory which predicts the amount of ^{13}N produced has been advanced (76) and might easily be extended to the case where oxygen is also present when additional ^{13}N is produced by the reaction $^{16}O(p,\alpha)^{13}N$. The theory states that the ^{13}N production rate depends on the proton flux, which is proportional to the product of hydrogen density and proton-range, and on the carbon and oxygen concentration. The ^{13}N production also limits the determination of copper in lubricating oils, since ^{62}Cu has the same half-life as ^{13}N and since both radionuclides are positron emitters (77). Other secondary reactions initiated by "knock-on" particles have been observed and even applied (79,80). Aumann and Born (81) described a simple and rapid non-destructive procedure for determining ^{18}O abundances in hydrogen-containing

substances by the reaction $^{18}O(p, n)^{18}F$ initiated by neutron-proton recoil in a reactor. Reactions occurring in neutron irradiated samples of water and organic compounds (C, H, O, N) are: $^{14}N(n, 2n)^{13}N$; $^{13}C(p, n)^{13}N$; $^{12}C(p, \gamma)^{13}N$; $^{16}O(p, \alpha)^{13}N$; $^{14}N(p, \alpha)^{11}C$; $^{17}O(p, \gamma)^{18}F$. If the samples are enriched in deuterium the following reactions are possible: $^{12}C(d, n)^{13}N$; $^{13}C(d, 2n)^{13}N$; $^{16}O(d, \gamma)^{18}F$ and $^{18}O(d, 2n)^{18}F$.

3. *Second Order Reactions*

Two types of second order reactions occur: those which enhance the production of an activation product and those which decrease its "concentration". Reactions of the first type usually occur when a major constituent of the sample, or the matrix itself, and the trace element have adjacent atomic numbers. In this case, activation products of the major constituent may decay to a stable isotope of the trace element, adding to its concentration. Long irradiation times and large reactor fluxes will greatly enhance the production of the trace element. In section III, E, of Chapter 5 the theoretical aspect of the problem has already been discussed.

In equation (5.63) the number of interfering nuclides (4) was calculated:

$$N_4(t_b) = \frac{6.025 \times 10^{23} \theta_1}{A_1} \varphi^2 \sigma_1 \sigma_3 F_2 \lambda_2 \sum_{i=1}^{i=4} C_i \exp(-\Lambda_i t_b) \qquad (10.38)$$

where: θ_1 = isotopic abundance of nuclide (1) in element Z;
θ_3 = isotopic abundance of nuclide (3) in element $(Z \pm 1)$;
A_1, A_3 = atomic weight of element (1), (3);
$\varphi = \varphi_{reactor}$ = reactor neutron flux;
$\sigma_1, \sigma_3 = \sigma_{reactor}$ = isotopic activation cross section, expressed in terms of a reactor cross section, thus including resonance activation (see section I of this chapter).

The number of radioactive nuclei N_4', formed by direct activation of 1 μg of the element $(Z + 1)$ or $(Z - 1)$, which has to be determined in element Z can be calculated from equation (10.1):

$$N_4'(t_b) = \frac{6.025 \times 10^{17} \theta_3 \sigma_3 \varphi}{\Lambda_4 A_3} [1 - \exp(-\Lambda_4 t_b)] \qquad (10.39)$$

Hence, the apparent concentration (in ppm) of the element $(Z \pm 1)$, formed from element Z by second order reaction, can directly be calculated from the ratio N_4/N_4':

$$\text{ppm}(Z \pm 1) = \frac{A_3}{A_1} \frac{\theta_1}{\theta_3} \frac{\varphi \sigma_1 F_2 \lambda_2 \Lambda_4 \sum_{i=1}^{i=4} C_i \exp(-\Lambda_i t_b)}{1 - \exp(-\Lambda_4 t_b)} 10^6 \qquad (10.40)$$

From this equation appears that – in first approximation – the interference is proportional to the flux and to σ_1.

It can be shown by calculation, that the final result is practically independent from σ_3 (implicitly present in C_i), but that it is directly proportional to σ_1, so that resonance activation of nuclide (1) must be included, whereas it can be omitted for nuclide (3). It can also be shown that the apparent concentration is directly proportional to φ, as far as burn-up is negligible (e.g. $\Lambda_4 = \lambda_4 + \varphi\sigma_4 \approx \lambda_4$), so that numerical values for any flux can be deduced from the values given in Table 10.9.

Some forty cases of second order interferences can be expected. Ricci and Dyer (82) calculated the interference for 23 cases as a function of irradiation time. The above equations are tedious to solve by hand and often lead to loss in significance in performing the summations of the exponential terms $C_i \exp(-\Lambda_i t_b)$. To make the calculations, a computer has to be programmed in an adequate computer code. Simpler formulas can be derived in the following way: the number of nuclei N_2 formed per second after an irradiation time t_b is given by:

$$N_2 = \frac{N_1^0 \varphi \sigma_1}{\lambda_2} [1 - \exp(-\lambda_2 t_b)]; \ (\Lambda_2 \approx \lambda_2) \qquad (10.41)$$

The corresponding number of disintegrations of nuclei (2) per second is then given by $\lambda_2 N_2 = N_1^0 \varphi \sigma_1 [1 - \exp(-\lambda_2 t_b)]$. This also gives the number of (stable) nuclei (3), formed per second assuming $F_2 = 1$. The total number of atoms (3), formed after an irradiation time t_b is calculated by integration of the last equation:

$$N_3(t_b) = \int_0^{t_b} N_2 \, dt_b = N_1^0 \varphi \sigma_1 \left[t_b - \frac{1 - \exp(-\lambda_2 t_b)}{\lambda_2} \right] \qquad (10.42)$$

If $N_3(t_b)$ is expressed in ppm $(Z \pm 1)$ in the matrix $(N_1^0 = \theta_1 N^0)$ this equation can be written as

$$\text{ppm}(Z \pm 1)(t_b) = \theta_1 \varphi \sigma_1 10^6 \left[t_b - \frac{1 - \exp(-\lambda_2 t_b)}{\lambda_2} \right] \qquad (10.43)$$

For $T_{1/2}(2) > t_b$, $1 - \exp(-\lambda_2 t_b) \approx \lambda_2 t_b - \frac{\lambda_2^2 t_b^2}{2} + \ldots$,

TABLE 10.9

Second order interference in ppb ($\varphi_{th} = 10^{12}$ n cm^{-2} s^{-1}; $\varphi_e/\varphi_{th} = 1/10^4$)

Determination of	$t_b(e)$			Determination of	$t_b(e)$		
	10^3	10^4	10^5		10^3	10^4	10^5
P in Si (^{31}P)	7×10^{-5}	4×10^{-3}	0.13				
Cl in S (^{35}Cl)	2×10^{-4}			Eu in Sm (^{154}Eu)		12	800
Sc in Ca (^{45}Sc)		1.6×10^{-5}	1.6×10^{-3}		0.65	5	445 (M)
Mn in Cr (^{55}Mn)	3×10^{-3}	5×10^{-3}		Eu in Gd (^{154}Eu)		2.6×10^{-3}	0.28 (M)
Co in Fe (^{59}Co)			1.4×10^{-3}				
Cu in Ni (^{64}Cu)		4×10^{-6}		Tb in Gd (^{159}Tb)	2.5×10^{-3}	0.165	13.3 (M)
Zn in Cu (^{65}Zn)	7×10^{-3}	0.75	60	Ho in Dy (^{165}Ho)		925	35,700 (M)
Ga in Zn (^{70} Ga)	1.2×10^{-2}			Tm in Er (^{170}Tm)		7.6×10^{-3}	0.75 (M)
Ga in Zn (^{72}Ga)	5×10^{-4}	8×10^{-3}		Lu in Yb (^{176m}Lu)		0.71	123 (M)
Ga in Ge (^{72}Ga)	2×10^{-4}	2×10^{-3}		Lu in Hf (^{176m}Lu)	5×10^{-5}	6×10^{-3}	
As in Ge (^{76}As)	2×10^{-3}	0.18	4.4	Ta in Hf (^{180}Ta)	1.6×10^{-4}	1.6×10^{-2}	1.6
	5×10^{-3}	0.39	11 (D)	W in Re (^{187}W)	4×10^{-3}	0.4	
Y in Sr (^{90}Y)		1.3×10^{-4}	1.3×10^{-3}	Re in W (^{188}Re)	5.2×10^{-5}	5.2×10^{-4}	0.44
Sb in Sn (^{122}Sb)	1.8×10^{-4}	1.6×10^{-2}	1.4	Re in W (^{188}Re)	3.5×10^{-2}	4.6	500
Sb in Sn (^{124}Sb)		5×10^{-3}	0.9	Ir in Pt (^{191}Ir)			1×10^{-3}(G)
La in Ba (^{140}La)	8×10^{-3}	0.7	22	Ir in Os (^{192}Ir)		5×10^{-3}	5 (G)
Ce in La (^{141}Ce)	3.4×10^{-3}	0.73	67 (M)	Ir in Os (^{194}Ir)		0.12	13 (G)
Pr in Co (^{140}Pr)		1.1×10^{-3}	0.14 (M)	Au in Pt (^{198}Au)		4×10^{-3}	3.8 (G)
				Tl in Hg (^{204}Tl)		1.2×10^{-3}	1.2

* Based on Ricci and Dyer (82); (M): D. L. Massart (71); (D) R. Donove (16); (G) R. Gijbels (83).

hence:

$$\text{ppm } (Z \pm 1)(t_b) \approx 0.5 \times 10^6\, \theta_1 \varphi \sigma_1 \lambda_2 t_b^2 \text{ (parabola)} \qquad (10.44)$$

For $T_{1/2}(2) \ll t_b$, $1 - \exp(-\lambda_2 t_b) \approx 1$, hence:

$$\text{ppm } (Z \pm 1)(t_b) \approx \theta_1 \varphi \sigma_1 10^6 \left(\frac{\lambda_2 t_b - 1}{\lambda_2}\right) \approx 10^6 \theta_1 \varphi \sigma_1 t_b \qquad (10.45)$$

(straight line)

These very simple formulas give, of course, only approximate results (order of magnitude), but they avoid laborious computer work.

Another algorithm has been proposed for fast and accurate calculations, without the need of a computer with high precision arithmetic (89). A compilation of 65 cases, of interest for neutron activation analysis, has been published (90,91).

Numerical data, taken from Ricci and Dyer (82), Massart (71), De Neve (16) and Gijbels (83) are summarized in Table 10.9, assuming $\varphi_{th} = 10^{12}$ n cm^{-2} s^{-1} and including resonance activation (for $\varphi_e/\varphi_{th} \approx 1/10$). As appears from Table 10.9, the second order interference is negligible in most cases, although it can introduce considerable errors (see, e.g. Re in W, Ho in Dy, Ir in Os).

Moreover, it must be borne in mind that the table assumes a flux of 10^{12} n cm^{-2} s^{-1} only. In the determination of As in transistor-grade germanium (~10 ppb As) at an irradiation of 10 h at 10^{14} n cm^{-2} s^{-1}, an apparent content of 200 ppb will be found, i.e. a factor of 20 too high. The interfering reaction may thus quite well limit the sensitivity of the analysis. In some cases different calculated values are tabulated, e.g. for As in Ge. This is due to a different value for σ_1 (Ricci 0.24 b; De Neve 0.6 b). An experimental study of the second order interference by De Neve (16) indicated that the best agreement between experiment and calculation is obtained for $\sigma_1 = 0.48$ b. Gijbels and Hoste (83) investigated experimentally the second order reaction ^{190}Os(n, γ)^{191}Os $\xrightarrow{\beta^-}$ ^{191}Ir(n, γ)^{192}Ir for irradiations of 1–10 days at a flux of 4×10^{11} n cm^{-2} s^{-1}. From the results an estimate of the resonance activation integral for ^{190}Os could be made (no literature data available). Normally, an experimental study of second order interference is only possible when starting from high purity materials, such as transistor grade germanium (9 ppb As), purified osmium (< 5 ppb Ir), etc. Other experimental results have been described (92).

In the above discussion, only reactions of the general form (n, γ) β

(n, γ) or (n, γ, EC, β^+ (n, γ) were considered. Other reactions can also interfere such as ^{164}Dy(n, γ)^{165}Dy(n, γ)^{166}Dy $\xrightarrow{\beta^-}$ ^{166}Ho together with ^{164}Dy(n, γ)^{165}Dy $\xrightarrow{\beta^-}$ ^{165}Ho(n, γ)^{166}Ho.

A second type of second order reactions decreases the "concentration" of the activation product. Tables to correct for the burn-up of a radioactivation product at high fluxes were calculated by Maslov (68).

Some radionuclides produced by (n, γ) reactions having a high cross section are ^{165}Dy (5000 b), ^{198}Au (26,000 b), ^{124}Sb (2000 b), ^{182}Ta (17,000 b), ^{14}C (200 b). The best known example is ^{197}Au(n, γ)^{198}Au(n, γ) ^{199}Au.

By applying the Bateman–Rubinson equation for transformations in a neutron flux (see Chapter 5) it can be shown that after an irradiation of 30 h at a flux of 10^{14} n cm^{-2} s^{-1}, 13% of the radioactive disintegrations in the gold sample occurs as ^{199}Au. Some experimental results are given by El Guebeily (84). After an irradiation of 50 h at 1.1×10^{13} n cm^{-2} s^{-1} the experimental ^{199}Au/^{198}Au ratio was 1.72%. For activation analysis purposes, there is little if any error introduced, if the comparator method is used, since the same reaction occurs in the comparator. If, however, the absolute assay method, or the "single comparator method" of Girardi (85) is used, this effect must be considered.

Finally, second order interference is not expected with fast neutrons, since their interaction cross section is too small.

4. *Primary Reactions Yielding Another Isotope of the Element to be Determined*

If cobalt is determined in nickel, not only ^{60}Co is formed, but also ^{58}Co from the reaction ^{58}Ni(n, p). Obviously, ^{60}Co and ^{58}Co cannot be separated by chemical means. Moreover, both radionuclides are very long-lived. Having different γ-energies, they can be measured selectively. As for a given irradiation position (given ratio thermal/fast flux) the ratio ^{60}Co/^{58}Co is directly proportional to the cobalt content in nickel, no flux monitoring is required, so that the above (n, p) reaction is actually not an interference, but yields a helpful internal standard. For low cobalt contents, the irradiation is carried out in a well thermalized neutron flux, to avoid too unfavourable ^{60}Co/^{58}Co activity ratios (86).

For contents <0.1 ppm Co, interference from the reaction ^{60}Ni(n, p)^{60}Co is possible.

A second example is the determination of arsenic in germanium. The nuclear reaction ^{76}Ge(n, γ)$^{77(m)}$Ge gives rise to ^{77}As with a half-life of 39 h (*cf.* ^{76}As : 26 h). The ^{76}As/^{77}As ratio in the radiochemically separated arsenic fraction is again directly proportional to the arsenic content in germanium. Hence no corrections for flux variations or chemical yield are necessary (see section II, B, 4c (4) of this chapter). The main difficulty arises from the very high ^{77}As activity as compared to the low ^{76}As activity ($\sim 10^4$ at the 1 ppm As level). Consequently the low-energy γ- or β-radiation of ^{77}As can interfere with the measurement of ^{76}As by pile up, both in γ-spectrometric and β-spectrometric techniques, so that absorbers (0.5 cm Pb and 270 mg. cm^{-2} Al respectively) must be used (56).

The same pile-up problem was found when determining gold (^{198}Au) in platinum, which gives rise to the radioactive ^{199}Au daughter of comparable half-life (54). At the 1 ppm gold level, the ^{199}Au/^{198}Au ratio was also $\sim 10^4$. A lead absorber (2.2 g. cm^{-2}) reduced strongly the ^{199}Au activity (transmission $\sim$16% for 208 KeV, $\sim$3% for 158 KeV and X-ray), whereas the 411 KeV γ-ray of ^{198}Au was reduced to 68% only, so that for 1 ppm the ratio ^{199}Au (158 or 208 KeV)/^{198}Au (411 KeV) becomes $\sim$150.

(D) Different Counting Efficiency

If the activated species is a pure β-emitter, it is normally counted with an end window counter after carrier addition and precipitation. If the β-energy is low, different problems arise, such as self absorption, self scattering and backscattering. The precipitates must, therefore, be in the same form and in the same geometrical condition and have the same weight for standards and samples.

In the case of low energy γ- or X-rays absorption is also possible.

Example: If ^{191}Os is distilled and the distillate absorbed in a suitable liquid, such as HBr, its activity (65 KeV X-ray + 129 KeV γ-ray) cannot directly be compared with that of a standard in the same volume of water.

Indeed, in Figure 10.10 the peak heights in the γ-spectrum of ^{191}Os are represented as a function of % HBr for a liquid source of 100 ml. The strong X-ray absorption is apparent (54).

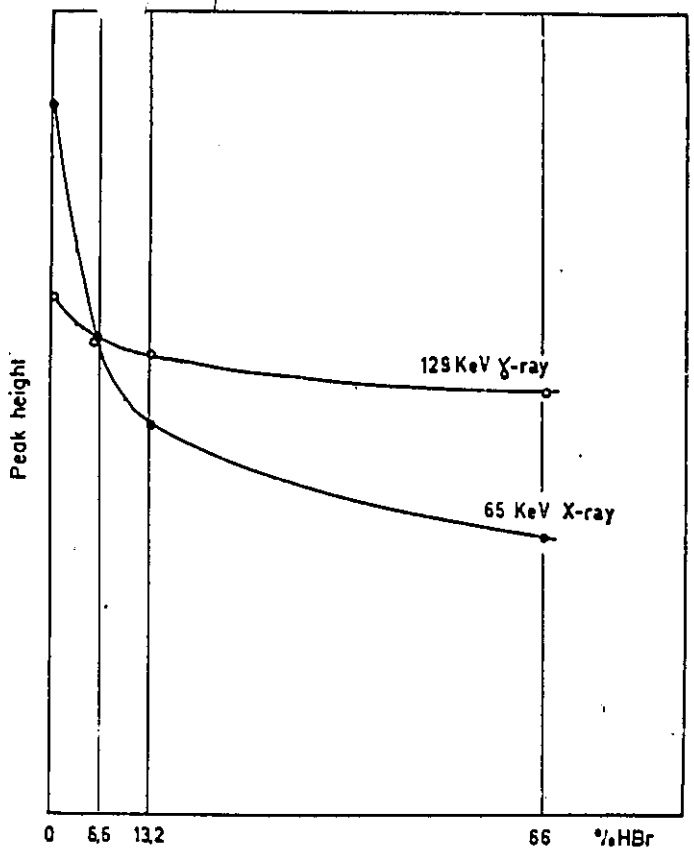

Fig. 10.10 Peak heights of 65 keV X-ray and 129 keV γ-ray (^{191}Os) as a function of % HBr in a liquid radioactive source of 100 ml.

As shown in Chapter 7, the samples and the "standards" are automatically counted in the same conditions, if an addition method is applied. Problems concerning the preparation of standards are also discussed in Chapter 7.

(E) Dead-Time Corrections

1. *General Considerations*

If the activity of the standard differs considerably from that of the fraction, isolated from the sample, systematic errors are possible due to different relative count losses. If possible, the activities for standards and samples should be of the same order of magnitude. Correction is however possible if the dead-time of the counting equipment is known. The overall dead-time depends on the dead-time of the detector, on the finite time constant of the amplifier, on the pulse-shaping circuits, on the scaler, etc. Modern scalers are very fast, bandwidths of 2 MHz are common. This means, in practice, that counting rates (statistical bursts!) of ca. 10^6 counts/m are possible without losses as far as the scaler is concerned. The count losses for G.M. tubes, integral gamma counters and single-channel analyzers can be calculated using equations (6.20) to (6.24), on condition that the dead-time of the equipment is known. A typical value for G.M. counting is 100 μs/count and for integral gamma counting 1–2 μs/count. In the latter case, a correction of ca. 1% may be required for 500,000 cpm or less. An average resolving time of 10 μs/count is common for single-channel analyzers. Counting rates should preferably not exceed ca. 500,000 cpm.

In many pulse height analyzers the resolving time is not constant but depends on the shape of the spectrum being measured, particularly in the case of analog to digital conversion (A.D.C).

From equation (6.36) it follows that multichannel analyzers have an average dead-time per recorded count given by:

$$\tau = k_1 + k_2 i_{av} \text{ (s/count)} \tag{10.46}$$

where k_1 is a constant due to memory cycle storage time (typically 10 μs/count), k_2 another constant due to spacing between address pulses (typically 0.5 μs/count/channel) and i_{av} the average channel number, depending on the shape of the spectrum:

$$i_{av} = \frac{\sum^{n} i c_i}{\sum^{n} c_i} \text{ (channel)} \tag{10.47}$$

where c_i is the number of counts recorded in channel i. When counting in 200 channels, the average channel i_{av} is generally situated between channel 20 and 100. Hence one can expect a τ value between 20 and 80 μs/count. With fast analog to digital converters (100 MHz oscillator frequency), τ values of 3.5 μs/count for 123 channels and 13 μs/count for 1024 channels can be obtained. Sometimes a fixed conversion time is used, e.g. 20 μs/count.

The total dead-time of a counting

$$DT = \tau c' \text{ (seconds)} \tag{10.48}$$

during a counting (clock) time CT depends on τ (shape of the spectrum) and on the total number of counts c' recorded.

The instantaneous dead-time IDT is defined by

$$IDT = \tau R' \text{ (no dimension)} \tag{10.49}$$

where R' is the observed counting rate (cps).

One defines a fractional dead-time FDT

$$FDT = DT/CT = (CT - LT)/CT \tag{10.50}$$

where DT = total dead time, CT = clock time and LT = total life time. Similarly, a fractional life-time $FLT = LT/CT$ can be defined. The FDT (and/or the FLT), expressed in %, is indicated on a galvanometer for most multichannel analyzers.

The life-timer is an electronic circuit which stops the timer during the pulse height analysis and memory storage and thus automatically corrects for count losses (life-time mode of counting). Depending on the instrument used, the life-time mode of counting may be in error by ca. +1% at gross rates of ca. 400,000 cpm, by ca. +2% at gross rates of ca. 600,000 cpm and by ca. +4% at gross rates of 10^6 cpm. This corresponds typically with fractional dead-times of ca. 20, 30 and 40% (200 channels). The dead-time losses, caused by finite conversion and storage time, can be substantially reduced if the analyzer contains a temporary or buffer storage mechanism (87), but its calculation becomes more difficult, particularly if the buffer is capable of storing more than one signal.

This correction by counting during a longer clock time ($CT = LT + DT$) is obviously inadequate for short-lived radionuclides, which decay during the counting: more counts are lost at the beginning of the counting, than can be "recovered" at the end. Automatic correction for short-lived radionuclides is only reasonable at low fractional dead times and short counting times with regard to the half-life.

Three different cases can be distinguished (88):

counting a pure short-lived radionuclide;

counting a short-lived radionuclide in the presence of one or more long-lived activities;

counting several short-lived radionuclides in the presence of one or more long-lived activities.

2. *Counting a Pure Short-lived Radionuclide*

The general shape of the spectrum remains constant (1 radioisotope), hence τ = constant. At any time t, the relative counting rate loss is given by the instantaneous dead time IDT (t):

$$\frac{R(t) - R'(t)}{R(t)} = IDT(t) = \tau R'(t) \tag{10.51}$$

where $R(t)$ is the real number of pulses/s presented for pulse height analysis, and $R'(t)$ the observed counting rate (cps) at time t. Hence:

$$R'(t) = \frac{R(t)}{1 + \tau R(t)} \tag{10.52}$$

where $R(t) = R^0 \exp(-\lambda t)$. Equation (10.52) relates the real and the effective counting rate at time t.

The total number of counts c' recorded in a clock time CT is obviously

$$c' = \int_0^{CT} R'(t)\,dt = \int_0^{CT} \frac{R^0 \exp(-\lambda t)}{1 + \tau R^0 \exp(-\lambda t)}\,dt \tag{10.53}$$

Writing $1 + \tau R^0 \exp(-\lambda t) = u$ yields the solution of this integral:

$$c' = \frac{1}{\lambda \tau} \ln \frac{1 + \tau R^0}{1 + \tau R^0 \exp(-\lambda . CT)} \tag{10.54}$$

or

$$\exp(\lambda \tau c') = \frac{1 + \tau R^0}{1 + \tau R^0 \exp(-\lambda . CT)} = \exp(\lambda . DT) \tag{10.55}$$

since the total dead time is $DT = \tau c'$. Further:

$$1 + \tau R^0 = \exp(\lambda . DT) + \tau R^0 \exp[-\lambda(CT - DT)]$$

Remembering that $CT - DT = LT$ and $\tau = DT/c'$, one finds for R^0:

$$R^0 = \frac{\exp(\lambda . DT) - 1}{1 - \exp(-\lambda . LT)} \frac{c'}{DT} \tag{10.56}$$

This exact equation allows us to calculate the true counting rate R^0 at $t = 0$ from the observed number of counts c', on condition that CT and DT or LT (and λ) are known.

In Chapter ... it is shown that, after a counting (clock) time $CT = LT$, (assuming $DT = 0$) the true total number of counts c and the true counting rate R^0 at $t = 0$ are related by the equation:

$$R^0 = \frac{\lambda c}{1 - \exp(-\lambda \,.\, LT)} \tag{10.57}$$

From equations (10.56) and (10.57) it follows:

$$\frac{c'}{c} = \frac{\lambda \,.\, DT}{\exp(\lambda \,.\, DT) - 1} = \frac{\lambda(CT - LT)}{\exp[\lambda(CT - LT)] - 1} \tag{10.58}$$

This exact formula allows one to calculate the true total number of counts c from c', on condition that CT and LT (and λ) are known. LT is measured by the multichannel analyzer (in life-time mode of counting) and the corresponding CT measured with a simple chronometer. A special set-up is described by Junod (88) where the multichannel is used in clock-time mode of counting, whereas LT is measured by means of an exterior chronometer, which is operated by the life-timer circuit. This method has the advantage that CT can be preselected, e.g. $1T_{1/2}$, $2T_{1/2}$, independent of the activity of the radioactive source.

Note: for long-lived radionuclides, i.e. $CT/T_{1/2} \ll 1$, equation (10.58) is reduced to $c'/c = 1$. Hence, the life timer makes no error, due to the decay of the measured isotope.

Example: $CT = 2.50$ m; $LT = 2.25$ m; $DT = 0.25$ m; further $FDT = DT/CT = 0.25/2.50 = 10\%$ (=average value of the instantaneous dead time); $T_{1/2} = 1$ m, hence $\lambda = 0.693$ m^{-1}; $CT/T_{1/2} = 2.50$.

From equation (10.58) one calculates:

$$\frac{c'}{c} = \frac{0.693 \times 0.25}{\exp(0.693 \times 0.25) - 1} = 0.92$$

i.e. the result of the life-time mode of counting (c') is too low by 8% (see also Figure 10.11: $FDT = 10\%$ and $CT/T_{1/2} = 2.50$).

Note: FDT can also be estimated by reading the "dead-time" galvanometer of the analyzer at time $t \simeq CT/2$. The correction of c' can then be performed using Figure 10.11. This figure is also useful to choose a counting time which is sufficiently short to make no errors $> x\%$, for a given FDT.

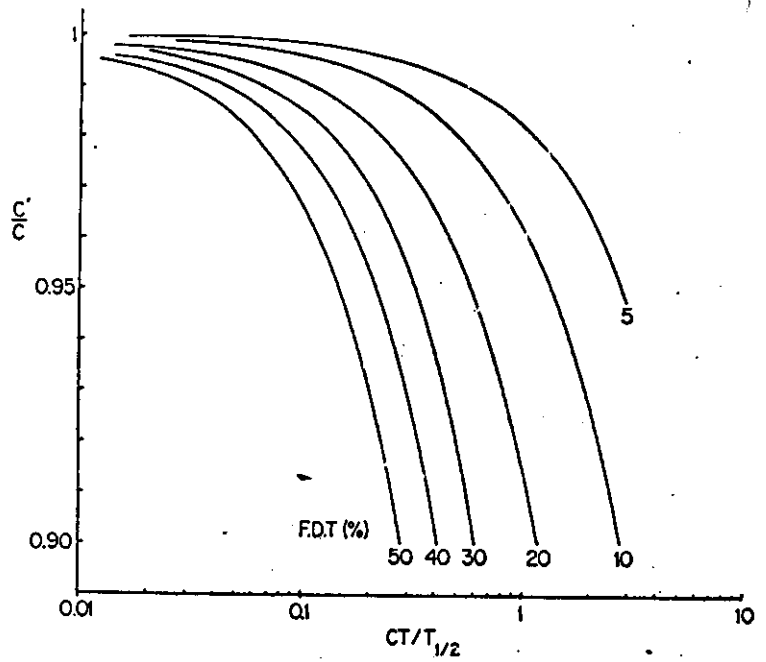

Fig. 10.11. Ratio of the observed number of counts (c') to true number of counts (c) as a function of $CT/T_{1/2}$ when using the life-time mode of counting. FDT = fractional dead-time (88).

3. *Counting a Short-lived Radionuclide in the presence of One or More Long-lived Radioactivities*

For the same FDT, the error made here will be smaller than in the foregoing case. This can easily be understood, since in the extreme case of a pure long-lived radionuclide, the life-timer makes no error due to decay. An exact treatment of this problem is given by Junod (88). Only a simplified discussion will be given here. Assuming $DT = 0$, the total number of counts c, observed in a clock time $CT = LT$ should be

$$c = \frac{R^0}{\lambda}[1 - \exp(-\lambda \,.\, LT)] \tag{10.57b}$$

In practice, however, $DT > 0$, hence one integrates from 0 to CT, but records only a fraction LT/CT, assuming that the dead-time is

almost completely due to the long-lived species. Thus:

$$c' = \frac{R^0}{\lambda}[1 - \exp(-\lambda \cdot CT)]\frac{LT}{CT} \qquad (10.59)$$

so that:

$$\frac{c'}{c} = \frac{1 - \exp(-\lambda \cdot CT)}{1 - \exp(-\lambda \cdot LT)}\frac{LT}{CT} \qquad (10.60)$$

Example: The same example as above will be used, assuming however that the dead time is completely due to the presence of a long lived species. From equation (10.60) one calculates:

$$\frac{c'}{c} = \frac{1 - \exp(-0.693 \times 2.5)}{1 - \exp(-0.693 \times 2.25)}\frac{2.25}{2.50} = 0.94$$

One remarks that the error made by the life-timer is somewhat smaller than for case 1, assuming the same FDT.

The counting of several short lived nuclides in the presence of several long lived ones is discussed by Junod (88). A general approach for calculating dead-time corrections with multichannel analyzers has been described by Schonfeld (94) and Gavron (95). Görner and Höhnel (96) presented an automatic correction, using one "corrector" per radionuclide to be counted.

(F) Other Errors

Until now, only experimental errors due to nuclear phenomena have been discussed. A second group of errors, which is not specific for activation analysis, is due to analytical procedures. Some of them will be mentioned.

1. *Failure to Remove Surface Contaminants from the Sample*

This may obviously be important when determining low oxygen concentrations with 14 MeV neutrons in samples having a chemically active surface, such as alkali metals, but also for Al, Ta, Nb, Cr, Pb, Zn, . . .

In the case of trace analysis for common elements by thermal activation, special care must be taken when preparing the samples before irradiation.

It should be borne in mind that often in a laboratory atmosphere 10^{12} atoms of Fe, Cu, Zn, Pb, Ca, Mg, Al, Si, . . . are present per cm³ of air. The sample may also be contaminated with nuclides recoiling from the container material due to the neutron capture process. Possible contamination can be eliminated by etching the solid samples after irradiation. These problems are discussed in Chapter 7.

After irradiation, radioactive contamination is possible if the isotope of interest is used in large quantities for other purposes.

2. *Incomplete Exchange Between Carrier and Trace Element*

A typical element where this problem occurs is iridium (93). The chemical effects of nuclear reactions must also be considered (Szilard-Chalmers effect). The activated element may give rise to a variety of chemical states and this can be important for irradiations of organic molecules, stable complex ions or oxygenated anions, especially for elements with a high electronegativity, such as the "metalloids", the noble metals or polyvalent elements in a high oxidation state. The Szilard effect often involves a valency change (lowering): Au(III) → Au, As(III) → As, Se(IV) → Se, Mn(VII) → Mn(IV), Cl(VII) → Cl^-, . . . Difficulties can also occur if carrier-free isotopes are formed, e.g. $^{32}S(n, p)^{32}P$, $^{130}Te(n, \gamma)^{131(m)}Te \xrightarrow{\beta^-} {}^{131}I$. Starting from aqueous solutions of TeO_2, I^-, IO^-, I_2, IO_3^- and IO_4^- are formed.

Therefore, the radiochemical purification should include as first step an oxidation-reduction cycle if the element has more than one valency.

A false chemical yield determination will also occur, if macro-quantities of other (nonactive) components contaminate the final precipitate of the trace impurity (determination of strontium in calcium-rich samples).

3. *Insufficient Decontamination in the Chemical Procedures*

If other elements are present in almost carrier-free concentrations, they are readily adsorbed on the precipitate of the investigated element. The radiochemical purity can mostly be checked by gammaspectrometry, particularly with a Ge(Li) detector, or by following the decay.

The behaviou. . such interfering elements is easier to control by adding "hold back" carriers.

4. *Faulty Preparation of "Comparators"*

In many cases, standards are used as dilute solutions. If such a solution is not freshly prepared, adsorption of the element of interest on the container walls (glass, pyrex, silica, polyethylene, . . .) is possible. As a general rule, the diluted solutions should be prepared just before use.

Most of the above errors can be kept to a minimum by maintaining high standards for laboratory techniques and for control of radioactive contamination. These sources of error are normally within the control of the analyst, except that, as ultimate sensitivity is approached, the magnitude of the error increases rapidly.

References

1. Stoughton, R. W., and Halperin, J., *Nucl. Sci. Engng.*, 6, 100 (1959).
2. Hughes, D. J., and Schwartz, R. B., *Neutron Cross Sections*, BNL-325 (1958).
3. Rose, H., *et al.*: *Proc. 2nd Internat. Conf. on the Peaceful Uses of Atomic Energy*, 16, 36, United Nations, New York (1958).
4. Cali, J. P., *et al.*: in *Modern Trends in Activation Analysis*, Proceedings of 1965 Internat. Conf., College Station, Texas (1966), p. 253.
5. Thode, H. G., *et al.*, *J. Am. Chem. Soc.*, 70, 3009 (1948).
6. Thode, H. G., *et al.*, *Can. J. Research*, 27B, 361 (1949).
7. Corless, J. T., and Winchester, J. W., *The Society for Applied Spectroscopy*, 2nd National Meeting, San Diego, Calif., Oct. 14–18 (1963).
8. Duckworth, H. E., *Mass Spectrometry*, Cambridge University Press, 1958.
9. Sautin, A., *Analyse par Activation d'un Mélange de Terres Rares*, Thesis, Lyon (1965).
10. De Goeij, J. J. M., *et al.*, *Radiochim. Acta*, 5, 117 (1966).
11. Born, H. J., and Aumann, D. C., *Radiochim. Acta*, 3, 62 (1964).
12. Leliaert, G., Hoste, J., and Eeckhaut, J., *Anal. Chim. Acta*, 19, 100 (1958).
13. Bowen, H. J. M., and Gibbons, D., *Radioactivation Analysis*, Clarendon Press, Oxford (1963).
14. Plumb, R. C., and Lewis, J. E., *Nucleonics*, 13(8), 42 (1955).
15. Lyon, W. S., Jr., *Guide to Activation Analysis*, Van Nostrand Comp., Princeton, New York (1964).
16. De Neve, R., De Soete, D., and Hoste, J., *Anal. Chim. Acta*, 36, 508 (1966).
17. Lepetit, H., Thesis Univ. Lyon, France, Lycen-6524 (1965).
18. Mott, W. E., and Orange, J. M., *Anal. Chem.*, 37, 1338 (1965).
19. Kenna, B. T., and Conrad, F. J., *Health Physics*, 12, 564 (1966).
20. Op De Beeck, J., *Journal of Radioanalytical Chemistry*, 1, 313 (19[illegible]
21. Girardi, F., Pauly, J., and Sabbioni, E., *Dosage de l'oxygène dans les produits organiques et les métaux par activation aux neutrons de 14 MeV*, EUR. 2290 f, Euratom, Brussels, 1965.
22. Adams, F., Thesis Univ. Ghent, Belgium (1963).
23. Høgdahl, O. T., *Neutron Absorption in Pile Neutron Activation Analysis*, MMPP-226-1 (Dec. 1962).
24. Case, K. M., *et al.*, *Introduction to the Theory of Neutron Diffusion*, I, Los Alamos, New Mexico (June 1953).
25. Niale, R. G., *Nucleonics*, 14(No. 3), 86 (1960).
26. Zweifel, P. F., *Nucleonics* 18(No. 11), 174 (1960).
27. Okada, M., *Int. J. Appl. Rad. Isotopes*, 13, 53 (1962).
28. Kamemoto, Y., *Int. J. Appl. Rad. Isotopes*, 15, 447 (1964).
29. Kenna, B. T., and Van Domelen, B. H., *Int. J. Appl. Rad. Isotopes*, 17, 47 (1966).
30. Høgdahl, O. T., *Radiochemical Methods of Analysis*, I, Proc. of Symp. Salzburg Oct. 19–23, 1964. p. 23, Internat. At. Energy Agency. Vienna 1965.
31. Reynolds, S. A., and Mullins, W. T., *Internat. J. Appl. Rad. Isotopes*, 14, 421 (1963).
32. Gilat, J., and Gurfinkel, Y., *Nucleonics*, 21 (No. 8), 143 (1963).
33. Männer, W., and Springer, T., *Nukleonik*, 1, 337 (1959).
34. Grün, A. E., *Nukleonik*, 3, 301 (1961).
35. Dalton, G. P., and Osborn, R. K., *Nucl. Sci. Engng.*, 9, 198 (1961).
36. Hanna, G. C., *Nucl. Sci. Engng.*, 15, 325 (1963).
37. Johnson, R. A., *Talanta*, 11, 149 (1964).
38. Bethe, H. A., *Rev. Mod. Phys.*, 9, 135 (1937).
39. Judd, A. M., *Neutron Flux Measurement by Resonance Activation of Foils*. British Report TRG 399(D) (1962).
40. Chernick, J., and Vernon, R., *Nucl. Sci. Engng*, 4, 649 (1958).
41. Brose, M., *Nukleonik*, 6, 134 (1964).
42. Eastwood, T. A., and Werner, R. D., *Nucl. Sci. Engng*, 13, 385 (1962).
43. Zijp, W. L., *Review of Activation Methods for the Determination of Intermediate Neutron Spectra*, RCN-40, Petten (Oct. 1965).
44. Eastwood, T. A., and Werner, R. D., *Can. J. Phys.*, 41, 1263 (1963).
45. Baumann, N. P., *Resonance Integrals and Self-Shielding Factors for Detector Foils*, DP-817 (Jan. 1963).
46. McGarry, E. D., *Trans. Am. Nucl. Soc.*, 7, 86 (1964).
47. Drake, M. K., *Nucleonics*, 24 (No. 8), 108 (1966).
48. Hoste, J., *Pure and Appl. Chem.*, 1, 99 (1960).
49. Gijbels, R., and Hoste, J., *Anal. Chim. Acta*, 32, 17 (1965).
50. Speecke, A., and Maes, K., *Radiochemical Methods of Analysis*, I. Proc. of Symp. Salzburg Oct. 19–23, 1964, p. 51. Intern. At. Energy, Vienna, 1965.
51. Spencke, H., Cless-Bernert, T., and Karlik, B., *Radiochemical Methods of Analysis*, I, Proc. of Symposium, Salzburg, Oct. 19–23, p. 197, 1964. I.A.E.A., Vienna 1965.
52. Leliaert, G., Hoste, J., and Eeckhaut, J., *Anal. Chim. Acta*, 19, 99 (1958).
53. Hoste, J., Bouten, P., and Adams, F., *Nucleonics*, 19 (No. 3), 118 (1961).

54. Gijbels, R [illegible]moirs of the *Koninklijke Vlaamse Academie voor Wetenschappen*, Letteren en Schone Kunsten van België, Klasse der Wetenschappen, XXIX, No. 96, Brussels 1967.
55. Gijbels, R., and Hoste, J., *Anal. Chim. Acta*, 41, 419 (1968).
56. De Soete, D., De Neve, R., and Hoste, J., *Modern Trends in Activation Analysis*, Proc. of 1965 International Conference, College Station, Texas 1966, p. 31.
57. Wood, D. E., and Roper, N. J., *Fast Neutron Activation Analysis for Silicon in Iron*, KN-65-140(R) (April 1965).
58. Van Grieken, R., Gijbels, R., and Hoste, J., *Anal. Chim. Acta*, in press.
59. Smales, A. A., and Loveridge, B. A., *Anal. Chim. Acta*, 13, 566 (1953).
60. Baumgartner, F., *Z. Elektrochemie*, 64, 1077 (1960).
61. Ördögh, M., Szabo, E., and Hegedus, D., *Radiochemical Methods of Analysis*, I, Proc. of Symposium, Salzburg, Oct. 19–23, p. 175, 1964, I.A.E.A., Vienna 1965.
62. Pauly, J., Babbioni, E., and Girardi, F., *Radiochemical Methods of Analysis*, II, Proc. of Symposium, Salzburg, Oct. 19–23, I.A.E.A., Vienna p. 297, 1965.
63. Mark, H. B., *et al.*, *Modern Trends in Activation Analysis*, Proceedings of 1965 Internat. Conf., College Station, Texas 1966, p. 107.
64. Roy, J. C., and Hawton, J. J., *Table of Estimated Cross Sections for* (n, p) (n, α) and (n, 2n) *Reactions in a Fission Neutron Spectrum*, AECL-1181 (1960).
65. Mellish, C. E., Payne, J. A., and Otlett, R. L., *Radioisotopes in Scientific Research*, 1, 35, Pergamon Press, London (1958).
66. Salmon, L., AERE, Harwell, Report AERE C/R 1324 (1954).
67. De Neve, R., De Soete, D., and Hoste, J., *Radiochim. Acta*, 5, 188 (1966).
68. Lux, F., *Radiochim. Acta*, 1, 20 (1962).
69. Maslov, I. A., *Radiochemical Methods of Analysis*, I, Proc. of Symp., Salzburg, Oct. 19–23, 1964. I.A.E.A., Vienna p. 41, 1965.
70. Dams, R., and Hoste, J., *Anal. Chim. Acta*, 41, 197 (1968); *Anal. Chim. Acta*, 41, 205 (1968).
71. Massart, D. L., Thesis Univ., Ghent, Belgium (1965).
72. De Boeck, R., Adams, F., and Hoste, J., *Anal. Chim. Acta*, 39, 270 (1967).
73. Koch, R. C., Activation Analysis Handbook, Academic Press, New York (1960).
74. Cuypers, M., and Cuypers, J., Gamma-Ray Spectra and Sensitivities for 14 MeV Neutron Activation Analysis, Texas A & M University, College Station, Texas (April 1966).
75. Gilmore, J. T., and Hull, D. E., *Modern Trends in Activation Analysis*, Proceedings of 1961 Internat. Conf., College Station, Texas 1962, p. 32.
76. Gilmore, J. T., and Hull, D. E., *Anal. Chem.*, 34, 187 (1962).
77. Gibbons, D., McCabe, W. J., and Olive, G., Proc. Symposium on *Radiochemical Methods of Analysis*, Salzburg, Austria, Oct. 19–23, 1964, I.A.E.A., Vienna, 1965.
78. Stehn, J. R., *Trans. Am. Nucl. Soc.*, 3, 467 (1960).
79. Amiel, S., and Peisach, M., *Anal. Chem.*, 34, 1305 (1962).
80. Glickstein, S. S., and Winter, R. G., *Nucl. Instrum. Methods*, 9, 226 (1960).
81. Aumann, D. C., and Born, H. J., Proc. Symposium on *Radioc[illegible]al Methods of Analysis*, Salzburg, Austria, Oct. 19–23, 1964, I.A.E.A., Vienna 1965.
82. Ricci, E., and Dyer, F. F., *Nucleonics*, 22, (No. 6), 45 (1964).
83. Gijbels, R., and Hoste, J., *Modern Trends in Activation Analysis*, Proceedings of 1965 Internat. Conf., College Station, Texas 1966, p. 129.
84. El Guebeily, M. A., *et al.*, *Radiochim. Acta*, 2, 217 (1964).
85. Girardi, F., Guzzi, G., and Pauly, J., *Anal. Chim.*, 37, 1085 (1965).
86. De Soete, D., and Hoste, J., *Radiochemical Methods of Analysis*, II, Proc. of Symp., Salzburg, Oct. 19–23, p. 91, 1964, I.A.E.A., Vienna 1965.
87. Chase, R. L., *Nuclear Pulse Spectrometry*, McGraw Hill, New York, 1961.
88. Junod, E., *Etudes d'Analyse par Activation* (Le Comptage de Radionuclides de Périodes Courtes, I (Parties A et B). Rapport CEA-R 2980, Paris, March 1966.
89. Maenhout, W., and Op de Beeck, J., *J. Radioanal. Chem.*, 5, 115 (1970).
90. Op de Beeck, J., *J. Radioanal. Chem.*, 3, 431 (1969).
91. Op de Beeck, J., *J. Radioanal. Chem.*, 4, 137 (1970).
92. Gijbels, R., De Vos, M., De Neve, R., and Hoste, J., *Radiochem. Radioanalyt. Letters*, 5, 145 (1970).
93. Kimberlin, J., Charoonratana, C., and Wasson, J., *Radiochim. Acta*, 10, 69 (1968).
94. Schonfeld, E., *Nucl. Instrum. Meth.*, 42, 213 (1966).
95. Gavron, A., *Nucl. Instrum. Meth.*, 67, 245 (1969).
96. Görner, W., and Höhnel, G., *Nucl. Intrum. Meth.*, 88, 193 (1970).